Extractions of unpolarised TMD distributions

Valerio Bertone
IRFU, CEA, Université Paris-Saclay

May 24, 2022, Transversity 2022, Pavia

Introduction

- The $q_{\rm T}$ distribution of a generic **high-mass** (Q) system has two main regimes:

  - for $q_{\rm T} \gtrsim$ Q **collinear factorisation** at *fixed perturbative order* is appropriate:

$$\left(\frac{d\sigma}{dq_T}\right)_{\rm f.o.} = \int_0^1 dx_1 \int_0^1 dx_2 f_1(x_1, Q) f_2(x_2, Q) \frac{d\hat{\sigma}}{dq_T} + \mathcal{O}\left[\left(\frac{\Lambda_{\rm QCD}}{Q}\right)^n\right]$$

  - for $q_{\rm T} \ll$ Q **transverse-momentum-dependent (TMD) factorisation** at *fixed logarithmic accuracy* is appropriate:

$$\left(\frac{d\sigma}{dq_T}\right)_{\rm res.} \overset{\rm TMD}{=} \sigma_0 H(Q) \int d^2\mathbf{b}_T e^{i\mathbf{b}_T\cdot\mathbf{q}_T} F_1(x_1, \mathbf{b}_T, Q, Q^2) F_2(x_2, \mathbf{b}_T, Q, Q^2) + \mathcal{O}\left[\left(\frac{q_T}{Q}\right)^m\right]$$

  - Collinear and TMD factorisations may eventually be **matched** to produce accurate results over the the full $q_{\rm T}$ spectrum.

Introduction

- The $q_{\rm T}$ distribution of a generic **high-mass** (Q) system has two main regimes:

  - for $q_{\rm T} \gtrsim$ Q **collinear factorisation** at *fixed perturbative order* is appropriate:

$$\left(\frac{d\sigma}{dq_T}\right)_{\rm f.o.} = \int_0^1 dx_1 \int_0^1 dx_2 f_1(x_1, Q) f_2(x_2, Q) \frac{d\hat{\sigma}}{dq_T} + \mathcal{O}\left[\left(\frac{\Lambda_{\rm QCD}}{Q}\right)^n\right]$$

  - for $q_{\rm T} \ll$ Q **transverse-momentum-dependent (TMD) factorisation** at *fixed logarithmic accuracy* is appropriate:

Main subject of this talk

$$\left(\frac{d\sigma}{dq_T}\right)_{\rm res.} \overset{\rm TMD}{=} \sigma_0 H(Q) \int d^2\mathbf{b}_T e^{i\mathbf{b}_T\cdot\mathbf{q}_T} F_1(x_1, \mathbf{b}_T, Q, Q^2) F_2(x_2, \mathbf{b}_T, Q, Q^2) + \mathcal{O}\left[\left(\frac{q_T}{Q}\right)^m\right]$$

  - Collinear and TMD factorisations may eventually be **matched** to produce accurate results over the the full $q_{\rm T}$ spectrum.

TMD factorisation

- TMD factorisation introduces two independent scales:
  - the **renormalisation scale μ**, originating from the UV renormalisation,
  - the **rapidity scale ζ**, originating from the cancellation of rapidity divergences.
- The respective **evolution equations** are:

$$\frac{\partial \ln F}{\partial \ln \sqrt{\zeta}} = K(\mu)$$

$$\frac{\partial \ln F}{\partial \ln \mu} = \gamma_F(\alpha_s(\mu)) - \gamma_K(\alpha_s(\mu)) \ln \frac{\sqrt{\zeta}}{\mu}$$

with: $$\frac{\partial K}{\partial \ln \mu} = -\gamma_K(\alpha_s(\mu))$$

- In addition, for small values of b_{T}, TMDs can be matched on coll. dists.:

$$F(\mu, \zeta) = C(\mu, \zeta) \otimes f(\mu)$$

- The solution is:

$$F(\mu,\zeta) = \exp\left\{K(\mu_0)\ln\frac{\sqrt{\zeta}}{\sqrt{\zeta_0}} + \int_{\mu_0}^{\mu}\frac{d\mu'}{\mu'}\left[\gamma_F(\alpha_s(\mu')) - \gamma_K(\alpha_s(\mu'))\ln\frac{\sqrt{\zeta}}{\mu'}\right]\right\} C(\mu_0,\zeta_0)\otimes f(\mu_0)$$

- Anomalous dims. and matching funcs. **perturbatively** computable.

TMD factorisation

- TMD factorisation introduces two independent scales:
  - the **renormalisation scale μ**, originating from the UV renormalisation,
  - the **rapidity scale ζ**, originating from the cancellation of rapidity divergences.

- The respective **evolution equations** are:

$$\frac{\partial \ln F}{\partial \ln \sqrt{\zeta}} = K(\mu)$$

$$\frac{\partial \ln F}{\partial \ln \mu} = \gamma_F(\alpha_s(\mu)) - \gamma_K(\alpha_s(\mu)) \ln \frac{\sqrt{\zeta}}{\mu}$$

with:

$$\frac{\partial K}{\partial \ln \mu} = -\gamma_K(\alpha_s(\mu))$$

- In addition, for small values of b_T, TMDs can be matched on coll. dists.:

Matching onto collinear

$$F(\mu, \zeta) = C(\mu, \zeta) \otimes f(\mu)$$

- The solution is:

Evolution (Sudakov) factor

$\mu_b = b_0 / b_T$

$$F(\mu, \zeta) = \exp\left\{ K(\mu_0) \ln \frac{\sqrt{\zeta}}{\sqrt{\zeta_0}} + \int_{\mu_0}^{\mu} \frac{d\mu'}{\mu'} \left[\gamma_F(\alpha_s(\mu')) - \gamma_K(\alpha_s(\mu')) \ln \frac{\sqrt{\zeta}}{\mu'} \right] \right\} C(\mu_0, \zeta_0) \otimes f(\mu_0)$$

- Anomalous dims. and matching funcs. **perturbatively** computable.

TMD factorisation

- When integrating over b_T, **large values of** b_T give raise to low scales in the **non-perturbative** region.

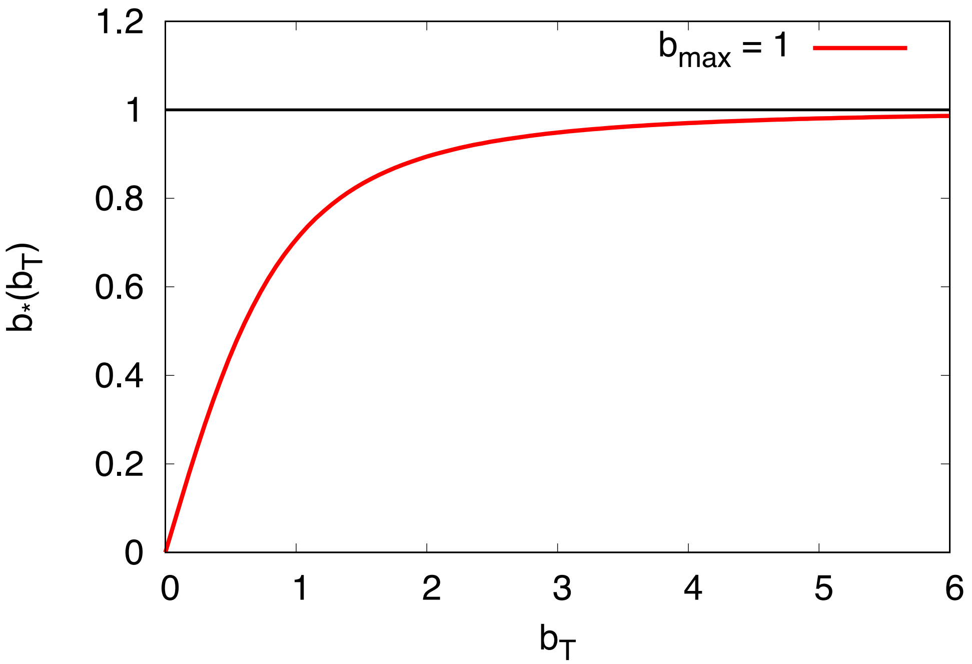

- Introduce the so-called **b*-prescription**:

$$b_*(b_T) = \frac{b_T}{\sqrt{1 + b_T^2/b_{\mathrm{max}}^2}}$$

- and rewrite:

$$F(x, b_T, \mu, \zeta) = \left[\frac{F(x, b_T, \mu, \zeta)}{F(x, b_*(b_T), \mu, \zeta)}\right] F(x, b_*(b_T), \mu, \zeta) \equiv f_{\mathrm{NP}}(x, b_T, \zeta) F(x, b_*(b_T), \mu, \zeta)$$

TMD factorisation

- When integrating over b_T, **large values of** b_T give raise to low scales in the **non-perturbative** region.

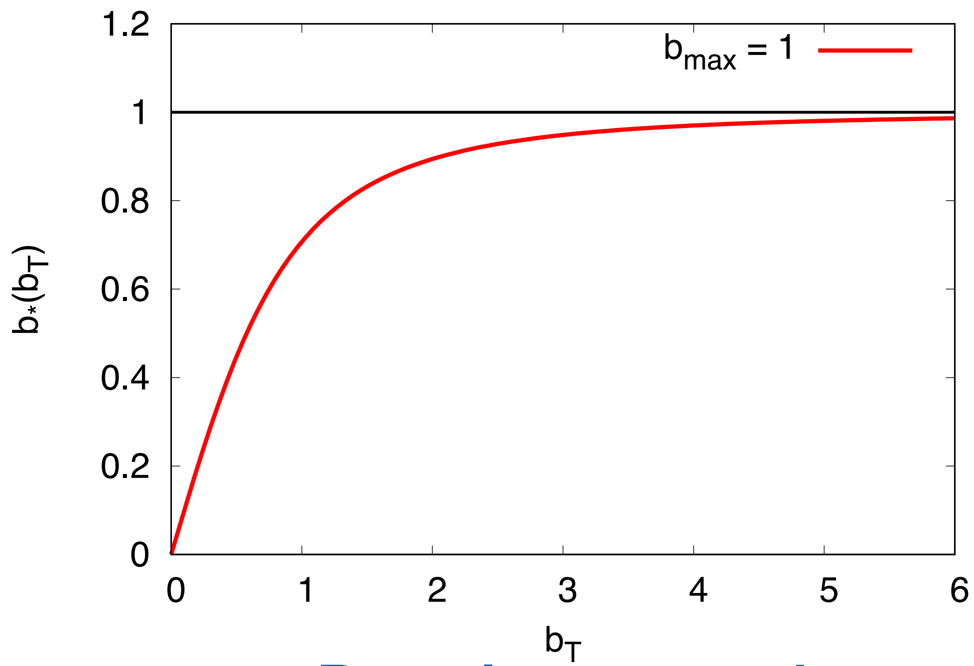

- Introduce the so-called **b*-prescription**:

$$b_*(b_T) = \frac{b_T}{\sqrt{1 + b_T^2/b_{\rm max}^2}}$$

- and rewrite:

$$F(x, b_T, \mu, \zeta) = \left[\frac{F(x, b_T, \mu, \zeta)}{F(x, b_*(b_T), \mu, \zeta)}\right] F(x, b_*(b_T), \mu, \zeta) \equiv f_{\rm NP}(x, b_T, \zeta) F(x, b_*(b_T), \mu, \zeta)$$

Purely perturbative

Non-perturbative, determine from data

- Properties of $f_{\rm NP}$:
  - has to go to **one** as b_T goes to zero: reproduce the fully perturbative regime,
  - has to got to **zero** as b_T becomes large: mimic the Sudakov suppression.

- Bottom line: avoidance of the non-perturbative region upon integration in b_T implies the presence of **both** b_*-prescription and $f_{\rm NP}$.

TMD factorisation

- Final expression:

$$
\begin{aligned}
F_{f/P}(x, \mathbf{b}_T; \mu, \zeta) \;=\; & \sum_j C_{f/j}(x, b_*; \mu_b, \mu_b^2) \otimes f_{j/P}(x, \mu_b) && : A \\
\times\; & \exp\left\{ K(b_*; \mu_b) \ln \frac{\sqrt{\zeta}}{\mu_b} + \int_{\mu_b}^{\mu} \frac{d\mu'}{\mu'} \left[\gamma_F - \gamma_K \ln \frac{\sqrt{\zeta}}{\mu'} \right] \right\} && : B \\
\times\; & \exp\left\{ g_{j/P}(x, b_T) + g_K(b_T) \ln \frac{\sqrt{\zeta_F}}{\sqrt{\zeta_{F,0}}} \right\} && : C
\end{aligned}
$$

- matching onto the collinear region at $b_T \ll 1/\Lambda_{QCD}$,
- factorises as *hard* (perturbative) and *longitudinal* (*i.e.* collinear, non-perturbative).

- CS and RGE evolution,
- evolution in μ and ζ,
- perturbative.

- avoid the Landau pole,
- f_{NP} accounts for the introduction of b_*,
- f_{NP} is non-perturbative thus **fit** to data.

Logarithmic counting

$$\left(\frac{d\sigma}{dq_T}\right)_{\text{res.}} \stackrel{\text{TMD}}{=} \sigma_0 H(Q) \int d^2 b_T e^{i b_T \cdot q_T} F_1(x_1, b_T, Q, Q^2) F_2(x_2, b_T, Q, Q^2)$$

$$F_f(x, b_T, \mu, \zeta) = \sum_j C_{f/j}(c, b_T; \mu_b, \zeta) \otimes f_j(x, \mu_b)$$
$$\times \exp\left\{ K(b_T, \mu_b) \ln\frac{\sqrt{\zeta}}{\mu_b} + \int_{\mu_b}^{\mu} \frac{d\mu'}{\mu'} \left[\gamma_F - \gamma_K \ln\frac{\sqrt{\zeta}}{\mu'}\right]\right\}$$

Accuracy	γ_K	γ_F	K	$C_{f/j}$	H	FFs/PDFs/α_s
LL	α_s	-	-	1	1	-
NLL	α_s^2	α_s	α_s	1	1	LO
NLL'	α_s^2	α_s	α_s	α_s	α_s	LO
N^{2}LL	α_s^3	α_s^2	α_s^2	α_s	α_s	NLO
N^{2}LL'	α_s^3	α_s^2	α_s^2	α_s^2	α_s^2	NLO
N^{3}LL	α_s^4	α_s^3	α_s^3	α_s^2	α_s^2	NNLO
N^{3}LL'	α_s^4	α_s^3	α_s^3	α_s^3	α_s^3	NNLO

Factorising processes

- Processes for which leading-power TMD factorisation has been **proven**:

Drell-Yan

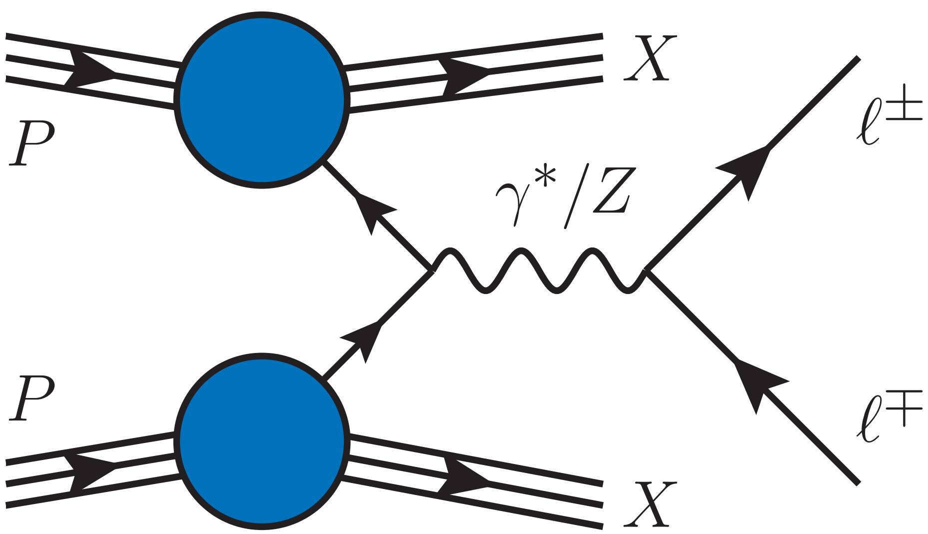

$$PP \longrightarrow \ell^\pm \ell^\mp \, X$$

- **Two** TMD **PDFs**:
- Lots of data:
  - low-energy: FNAL,
  - mid-energy: RHIC,
  - high-energy: Tevatron, LHC.

Semi-inclusive DIS

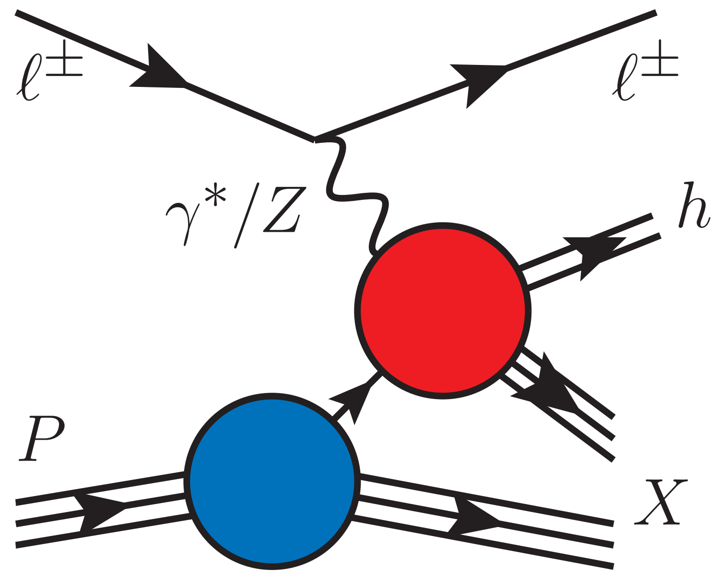

$$P\ell^\pm \longrightarrow \ell^\pm h \, X$$

- One TMD **PDF** one **FF**:
- many precise data points:
  - HERMES at DESY,
  - COMPASS at CERN.

e^+e^- annihilation

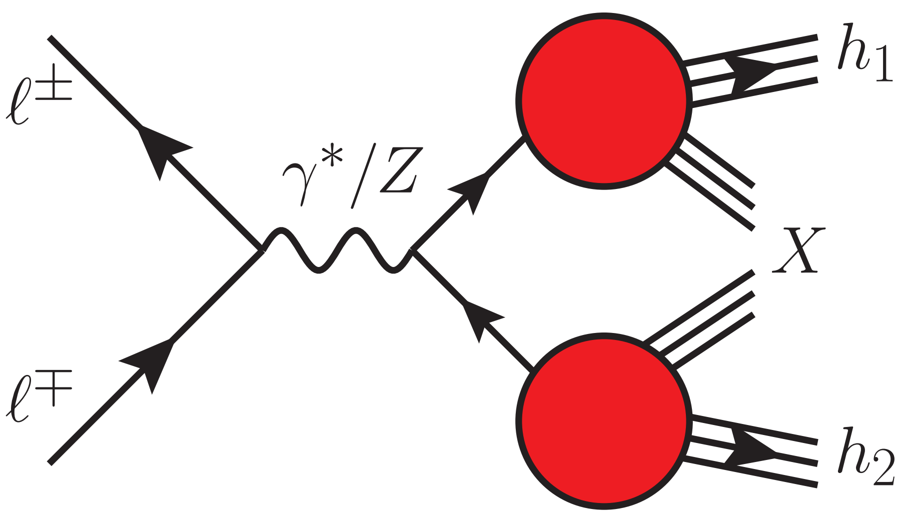

$$\ell^\pm \ell^\mp \to h_1 h_2 \, X$$

- **Two** TMD **FFs**:
- di-hadron prod. from:
  - BELLE at KEK,
  - BABAR at SLAC.

- Examples of other precesses:
  - thrust and p_{hT} distributions in single-hadron production in e^+e^-,
  - hadron-in-jet production,
  - …

Unpolarised TMD extractions

A selection of fits

	Accuracy	SIDIS	Drell-Yan	N. of points
DWS 1884, CERN-TH.3987/84	NLL	✘	✔	a few
BLNY 2003, hep-ph/0212159	NLL'-NNLL	✘	✔	116
Pavia 2013, arXiv:1309.3507	No evolution	✔	✘	1538 (HERMES)
Torino 2014, arXiv:1312.6261	No evolution	✔	✘	576 (H) 6284 (C)
DEMS 2014, arXiv:1407.3311	NNLL	✘	✔	223
Pavia 2017, arXiv:1703.10157	NLL	✔	✔	8059
SV 2017, arXiv:1706.01473	N^3LL	✘	✔ (LHC)	309
BSV 2019, arXiv:1902.08474	N^3LL	✘	✔ (LHC)	457
SV 2019, arXiv:1912.06532	$N^3LL^{(-)}$	✔	✔ (LHC)	1039
Pavia 2019, arXiv:1912.07550	N^3LL	✘	✔ (LHC)	353
Pia's talk, arXiv:2201.07114	N^3LL	✘	✔ (LHC)	507/309
MAPTMD 2022 (In preparation)	$N^3LL^{(-)}$	✔	✔ (LHC)	2031

Unpolarised TMD extractions

A selection of fits

	Accuracy	SIDIS	Drell-Yan	N. of points
DWS 1884, CERN-TH.3987/84	NLL	✘	✔	a few
BLNY 2003, hep-ph/0212159	NLL'-NNLL	✘	✔	116
Pavia 2013, arXiv:1309.3507	No evolution	✔	✘	1538 (HERMES)
Torino 2014, arXiv:1312.6261	No evolution	✔	✘	576 (H) 6284 (C)
DEMS 2014, arXiv:1407.3311	NNLL	✘	✔	223
Pavia 2017, arXiv:1703.10157	NLL	✔	✔	8059
SV 2017, arXiv:1706.01473	N^3LL	✘	✔ (LHC)	309
BSV 2019, arXiv:1902.08474	N^3LL	✘	✔ (LHC)	457
SV 2019, arXiv:1912.06532	$N^3LL^{(-)}$	✔	✔ (LHC)	1039
Pavia 2019, arXiv:1912.07550	N^3LL	✘	✔ (LHC)	353
Pia's talk, arXiv:2201.07114	N^3LL	✘	✔ (LHC)	507/309
MAPTMD 2022 (In preparation)	$N^3LL^{(-)}$	✔	✔ (LHC)	2031

Unpolarised TMD extractions

Many more studies and extractions…

- TMD fragmentation functions from e^+e^- data [2108.04182, 1704.08882]
- W production in pp collisions [2011.05351]
- Dijet and heavy-meson pair production in DIS [2008.07531, 2111.03703]
- Dijet production in pp collisions [*e.g.* 1807.07573]
- hadron-in-jet production [1612.04817]
- Model-independent prescription to extract TMDs [2201.07237]
- Parton-branching methods [*e.g.* 1804.11152]
- q_T-resummation based extractions [2203.05394]
- Study of the Sivers TMDs [1308.5003, 2004.14278, 2009.10710, 2103.03270]
- Pion TMDs [1907.10356]
- TMD flavour dependence [1807.02101]
- …

MAPTMD 2022

Dataset

- DY data:
  - fixed-target low-energy DY,
  - RHIC data,
  - LHC and Tevatron data,
  - selection cut $q_T / Q < 0.2$,
  - 484 data points.
- SIDIS data:
  - HERMES and COMPASS,
  - $P_{hT}|_{\max} = \min[\min[0.2Q, 0.5zQ] + 0.3 \text{ GeV}, zQ]$
  - $Q > 1.4$ GeV, $0.2 < z < 0.7$,
  - 1547 points.

Experiment	N_{dat}	Observable	$\sqrt{s}$ [GeV]	Q [GeV]	y or x_F	Lepton cuts	Ref.
E605	50	$Ed^3\sigma/d^3\boldsymbol{q}$	38.8	7 - 18	$x_F = 0.1$	-	[55]
E772	53	$Ed^3\sigma/d^3\boldsymbol{q}$	38.8	5 - 15	$0.1 < x_F < 0.3$	-	[51]
E288 200 GeV	30	$Ed^3\sigma/d^3\boldsymbol{q}$	19.4	4 - 9	$y = 0.40$	-	[56]
E288 300 GeV	39	$Ed^3\sigma/d^3\boldsymbol{q}$	23.8	4 - 12	$y = 0.21$	-	[56]
E288 400 GeV	61	$Ed^3\sigma/d^3\boldsymbol{q}$	27.4	5 - 14	$y = 0.03$	-	[56]
STAR 510	7	$d\sigma/d\|\boldsymbol{q}_T\|$	510	73 - 114	$\|y\| < 1$	$p_{T\ell} > 25$ GeV $\|\eta_\ell\| < 1$	-
PHENIX200	2	$d\sigma/d\|\boldsymbol{q}_T\|$	200	4.8 - 8.2	$1.2 < y < 2.2$	-	[52]
CDF Run I	25	$d\sigma/d\|\boldsymbol{q}_T\|$	1800	66 - 116	Inclusive	-	[57]
CDF Run II	26	$d\sigma/d\|\boldsymbol{q}_T\|$	1960	66 - 116	Inclusive	-	[58]
D0 Run I	12	$d\sigma/d\|\boldsymbol{q}_T\|$	1800	75 - 105	Inclusive	-	[59]
D0 Run II	5	$(1/\sigma)d\sigma/d\|\boldsymbol{q}_T\|$	1960	70 - 110	Inclusive	-	[60]
D0 Run II (μ)	3	$(1/\sigma)d\sigma/d\|\boldsymbol{q}_T\|$	1960	65 - 115	$\|y\| < 1.7$	$p_{T\ell} > 15$ GeV $\|\eta_\ell\| < 1.7$	[61]
LHCb 7 TeV	7	$d\sigma/d\|\boldsymbol{q}_T\|$	7000	60 - 120	$2 < y < 4.5$	$p_{T\ell} > 20$ GeV $2 < \eta_\ell < 4.5$	[62]
LHCb 8 TeV	7	$d\sigma/d\|\boldsymbol{q}_T\|$	8000	60 - 120	$2 < y < 4.5$	$p_{T\ell} > 20$ GeV $2 < \eta_\ell < 4.5$	[63]
LHCb 13 TeV	7	$d\sigma/d\|\boldsymbol{q}_T\|$	13000	60 - 120	$2 < y < 4.5$	$p_{T\ell} > 20$ GeV $2 < \eta_\ell < 4.5$	[64]
CMS 7 TeV	4	$(1/\sigma)d\sigma/d\|\boldsymbol{q}_T\|$	7000	60 - 120	$\|y\| < 2.1$	$p_{T\ell} > 20$ GeV $\|\eta_\ell\| < 2.1$	[65]
CMS 8 TeV	4	$(1/\sigma)d\sigma/d\|\boldsymbol{q}_T\|$	8000	60 - 120	$\|y\| < 2.1$	$p_{T\ell} > 15$ GeV $\|\eta_\ell\| < 2.1$	[66]
CMS 13 TeV	70	$d\sigma/d\|\boldsymbol{q}_T\|$	13000	76 - 106	$\|y\| < 0.4$ $0.4 < \|y\| < 0.8$ $0.8 < \|y\| < 1.2$ $1.2 < \|y\| < 1.6$ $1.6 < \|y\| < 2.4$	$p_{T\ell} > 25$ GeV $\|\eta_\ell\| < 2.4$	[53]
ATLAS 7 TeV	6 6 6	$(1/\sigma)d\sigma/d\|\boldsymbol{q}_T\|$	7000	66 - 116	$\|y\| < 1$ $1 < \|y\| < 2$ $2 < \|y\| < 2.4$	$p_{T\ell} > 20$ GeV $\|\eta_\ell\| < 2.4$	[67]
ATLAS 8 TeV on-peak	6 6 6 6 6 6	$(1/\sigma)d\sigma/d\|\boldsymbol{q}_T\|$	8000	66 - 116	$\|y\| < 0.4$ $0.4 < \|y\| < 0.8$ $0.8 < \|y\| < 1.2$ $1.2 < \|y\| < 1.6$ $1.6 < \|y\| < 2$ $2 < \|y\| < 2.4$	$p_{T\ell} > 20$ GeV $\|\eta_\ell\| < 2.4$	[68]
ATLAS 8 TeV off-peak	4 8	$(1/\sigma)d\sigma/d\|\boldsymbol{q}_T\|$	8000	46 - 66 116 - 150	$\|y\| < 2.4$	$p_{T\ell} > 20$ GeV $\|\eta_\ell\| < 2.4$	[68]
ATLAS 13 TeV	6	$(1/\sigma)d\sigma/d\|\boldsymbol{q}_T\|$	13000	66 - 113	$\|y\| < 2.5$	$p_{T\ell} > 27$ GeV $\|\eta_\ell\| < 2.5$	[54]
Total	484						

Experiment	N_{dat}	Observable	Channels	Q [GeV]	x	z	Phase space cuts	Ref.
HERMES	344	$M(x, z, \|\boldsymbol{P}_{hT}\|, Q)$	$p \to \pi^+$ $p \to \pi^-$ $p \to K^+$ $p \to K^-$ $d \to \pi^+$ $d \to \pi^-$ $d \to K^+$ $d \to K^-$	1 - $\sqrt{15}$	$0.023 < x < 0.6$ (6 bins)	$0.1 < z < 1.1$ (8 bins)	$W^2 > 10$ GeV^2 $0.1 < y < 0.85$	[46]
COMPASS	1203	$M(x, z, \boldsymbol{P}_{hT}^2, Q)$	$d \to h^+$ $d \to h^-$	1 - 9 (5 bins)	$0.003 < x < 0.4$ (8 bins)	$0.2 < z < 0.8$ (4 bins)	$W^2 > 25$ GeV^2 $0.1 < y < 0.9$	[72]
Total	1547							

MAPTMD 2022

Kinematic coverage

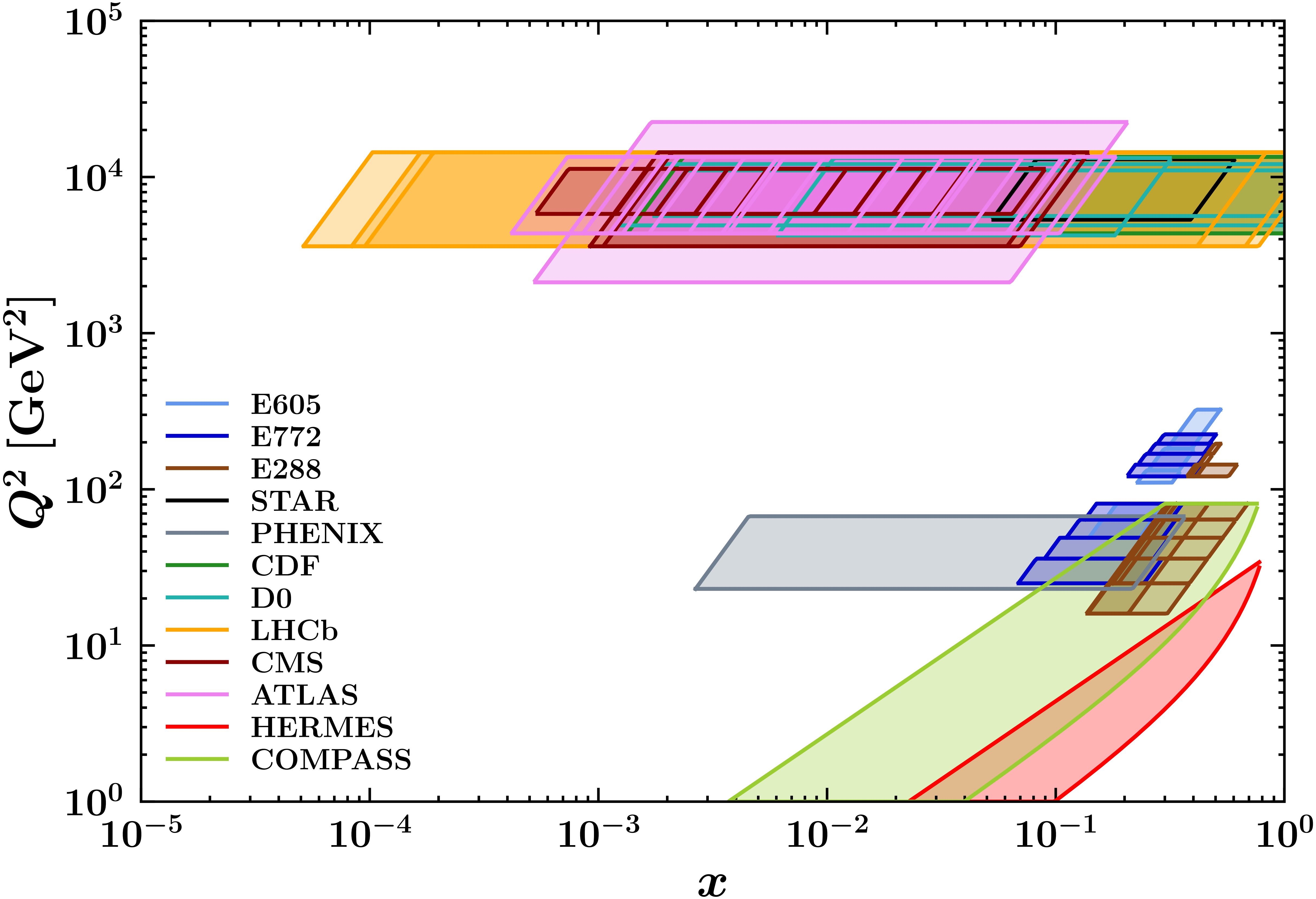

MAPTMD 2022

Main settings

- b_* prescription:

$$b_*(b_T) = b_{\max}\left(\frac{1-e^{-b_T^4/b_{\max}^4}}{1-e^{-b_T^4/b_{\min}^4}}\right)^{1/4} \quad \text{with} \quad \begin{cases} b_{\max} = 2e^{-\gamma_E} \\ b_{\min} = b_{\max}/Q \end{cases}$$

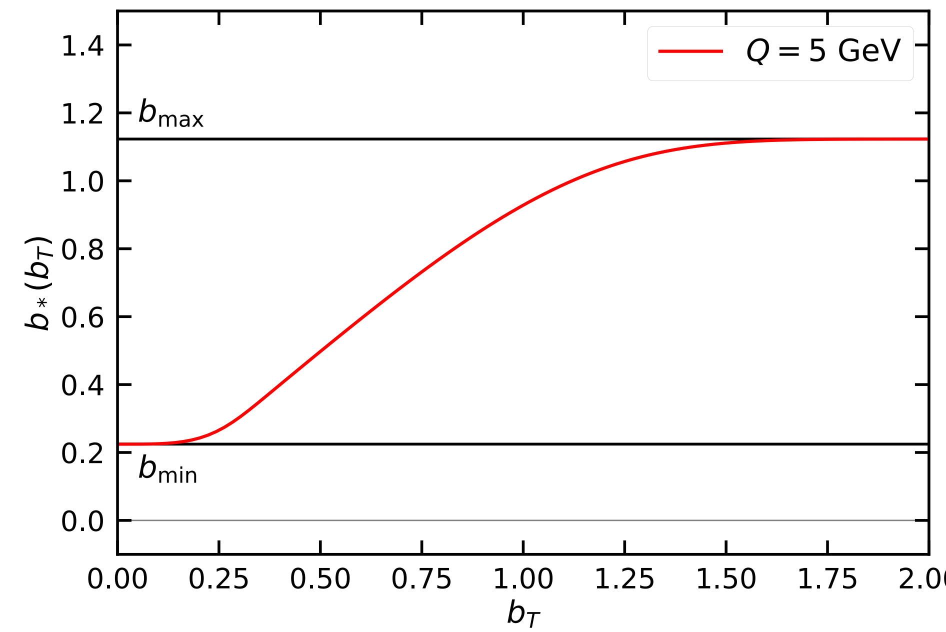

- Non-perturbative function $f_{\rm NP}$:
  - evolution: $g_K(\boldsymbol{b}_T^2) = -g_2^2\,\frac{\boldsymbol{b}_T^2}{2}$
  - PDFs:

$$f_{1\,NP}(x,\boldsymbol{b}_T^2;\zeta,Q_0) = \frac{g_1(x)\,e^{-g_1(x)\frac{\boldsymbol{b}_T^2}{4}} + \lambda^2\,g_{1B}^2(x)\left[1-g_{1B}(x)\frac{\boldsymbol{b}_T^2}{4}\right]e^{-g_{1B}(x)\frac{\boldsymbol{b}_T^2}{4}} + \lambda_2^2\,g_{1C}(x)\,e^{-g_{1C}(x)\frac{\boldsymbol{b}_T^2}{4}}}{g_1(x)+\lambda^2\,g_{1B}^2(x)+\lambda_2^2\,g_{1C}(x)}\left[\frac{\zeta}{Q_0^2}\right]^{g_K(\boldsymbol{b}_T^2)/2}$$

  - FFs:

$$D_{1\,NP}(z,\boldsymbol{b}_T^2;\zeta,Q_0) = \frac{g_3(z)\,e^{-g_3(z)\frac{\boldsymbol{b}_T^2}{4z^2}} + \frac{\lambda_F}{z^2}\,g_{3B}^2(z)\left[1-g_{3B}(z)\frac{\boldsymbol{b}_T^2}{4z^2}\right]e^{-g_{3B}(z)\frac{\boldsymbol{b}_T^2}{4z^2}}}{g_3(z)+\frac{\lambda_F}{z^2}\,g_{3B}^2(z)}\left[\frac{\zeta}{Q_0^2}\right]^{g_K(\boldsymbol{b}_T^2)/2}$$

$$g_{\{1,1B,1C\}}(x) = N_{\{1,1B,1C\}}\frac{x^{\sigma_{\{1,2,3\}}}(1-x)^{\alpha^2_{\{1,2,3\}}}}{\hat{x}^{\sigma_{\{1,2,3\}}}(1-\hat{x})^{\alpha^2_{\{1,2,3\}}}} \qquad g_{\{3,3B\}}(z) = N_{\{3,3B\}}\frac{(z^{\beta_{\{1,2\}}}+\delta^2_{\{1,2\}})(1-z)^{\gamma^2_{\{1,2\}}}}{(\hat{z}^{\beta_{\{1,2\}}}+\delta^2_{\{1,2\}})(1-\hat{z})^{\gamma^2_{\{1,2\}}}}$$

- 11 (PDFs) + 9 (FFs) + 1 (evol): **21 free parameters** to fit to data.
- Perturbative accuracies: **N^{3}LL(-)**.
- **Monte Carlo** method for the experimental error propagation.

MAPTMD 2022

Normalisation of SIDIS

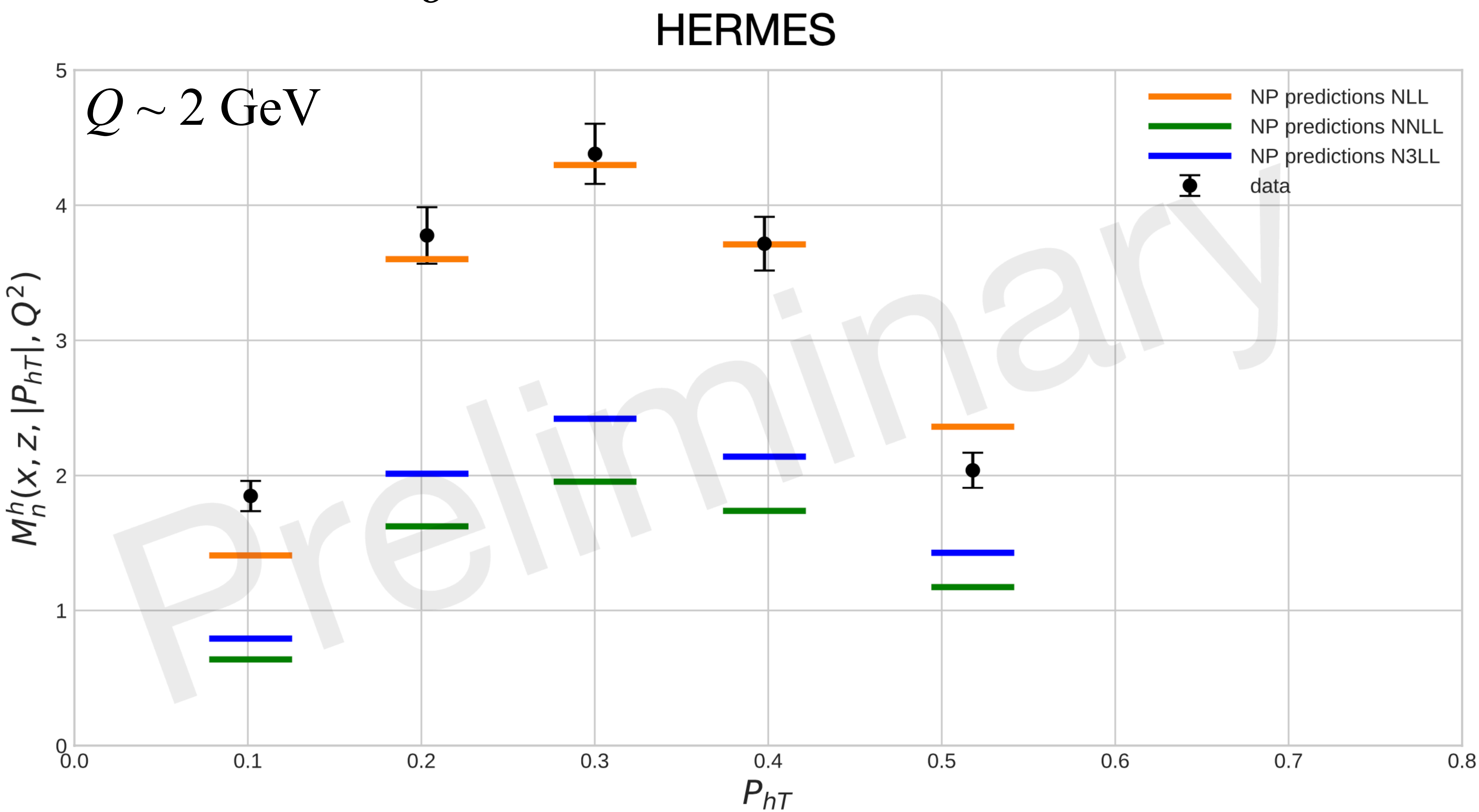

- Description of SIDIS multiplicities considerably worsens moving from NLL to higher perturbative orders.

MAPTMD 2022

Normalisation of SIDIS

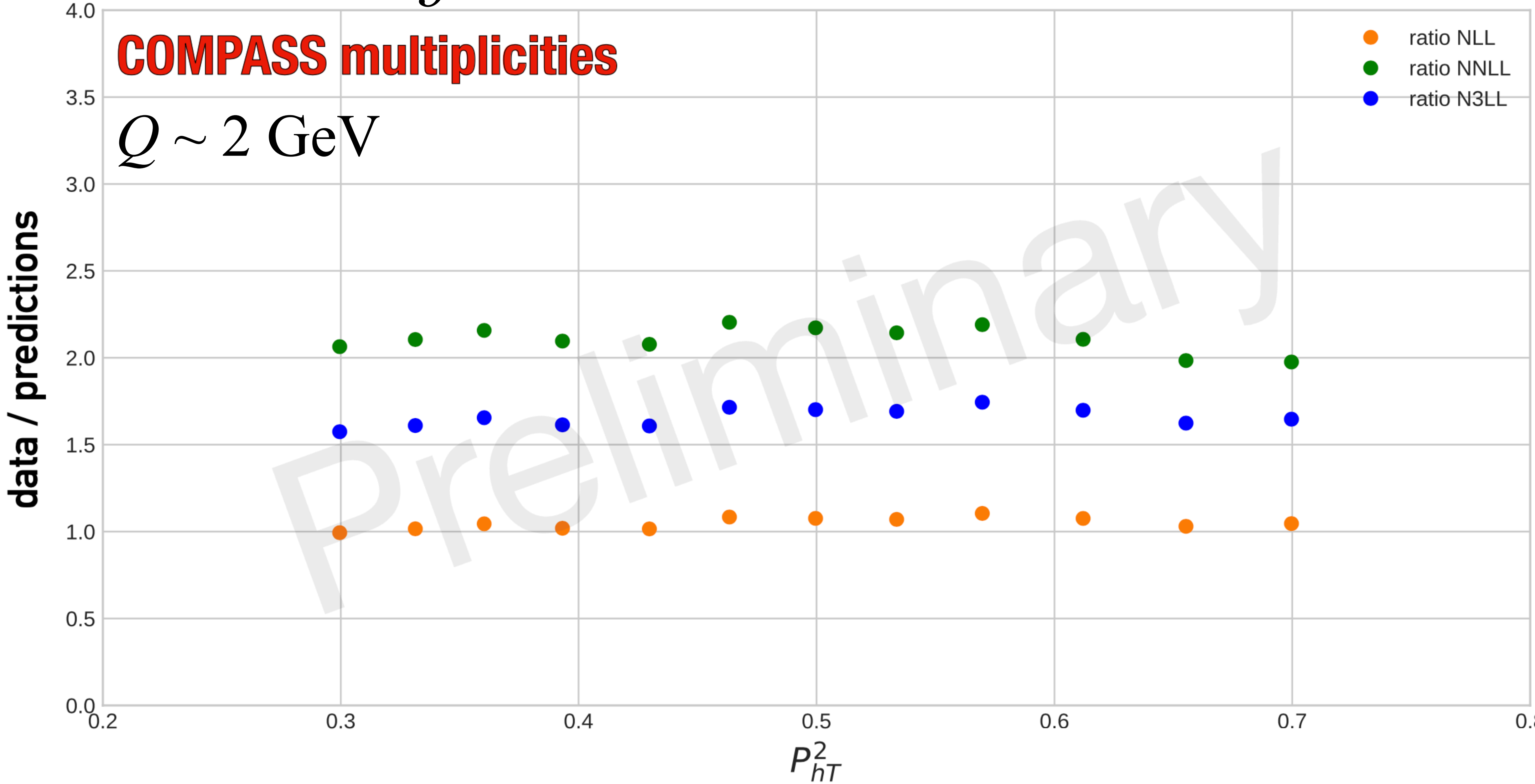

- Normalisation problem already observed in the literature.
- Large perturbative corrections particularly to the hard function:

$$H(Q) = 1 + \frac{\alpha_s(Q)}{4\pi} C_F \left(-16 + \frac{\pi^2}{3} \right) + \mathcal{O}(\alpha_s^2)$$

MAPTMD 2022

Normalisation of SIDIS

- SIDIS multiplicity: $M(x, z, P_{hT}, Q) = \frac{d\sigma}{dxdQ\color{red}{dzdP_{hT}}} \Big/ \frac{d\sigma}{dxdQ}$
- The SIDIS cross section integrated over P_{hT} ($d\sigma/dxdQ\color{red}{dz}$) is ok.

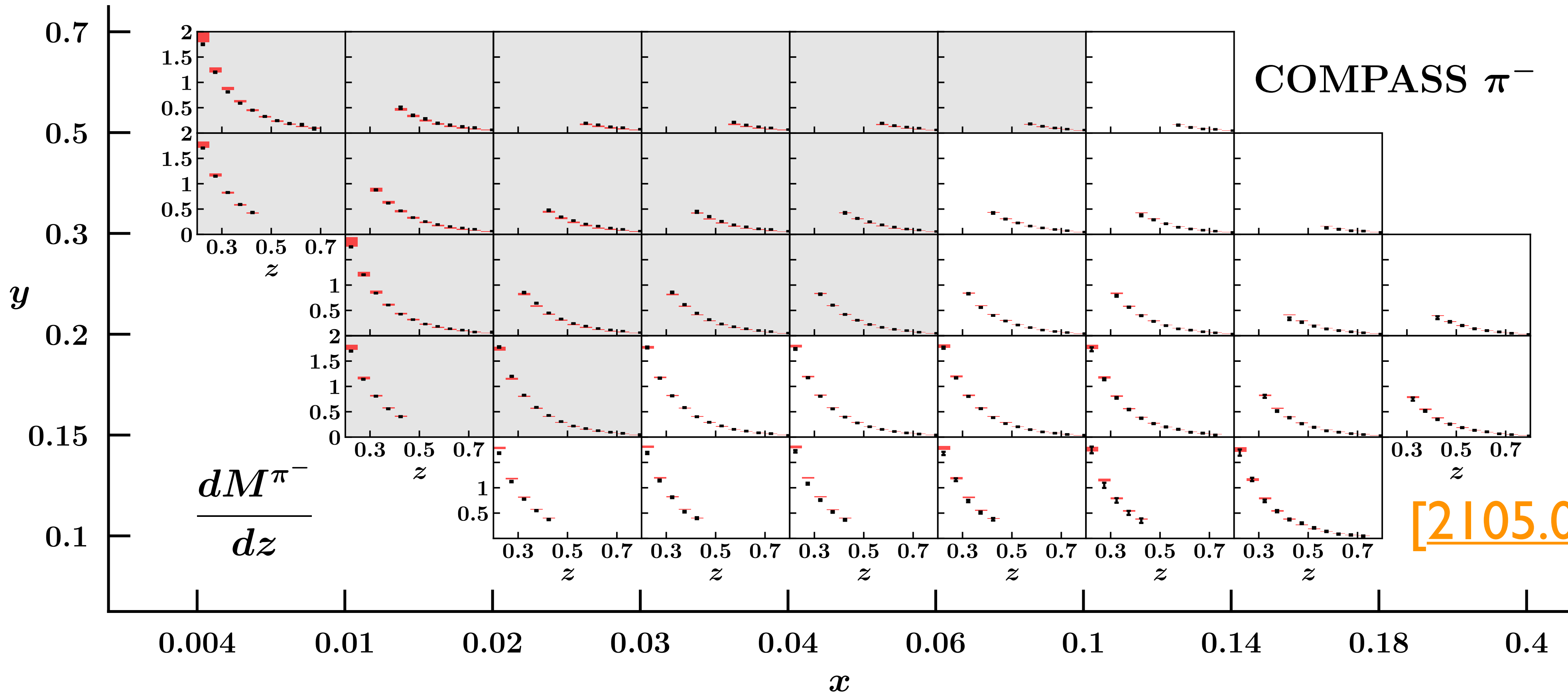

[2105.08725]

- Normalise predictions such that integral over P_{hT} gives $d\sigma/dxdQ\color{red}{dz}$:

$$M(x, z, P_{hT}, Q) = \color{red}{\mathcal{N}} \frac{\frac{d\sigma}{dxdQ\color{red}{dzdP_{hT}}}}{\frac{d\sigma}{dxdQ}} \qquad \mathcal{N} = \frac{\frac{d\sigma}{dxdQ\color{red}{dz}}}{\int dP_{hT} \frac{d\sigma}{dxdQ\color{red}{dzdP_{hT}}}}$$

- Theoretically justified normalisation and **not fitted**.

MAPTMD 2022

Normalisation of SIDIS

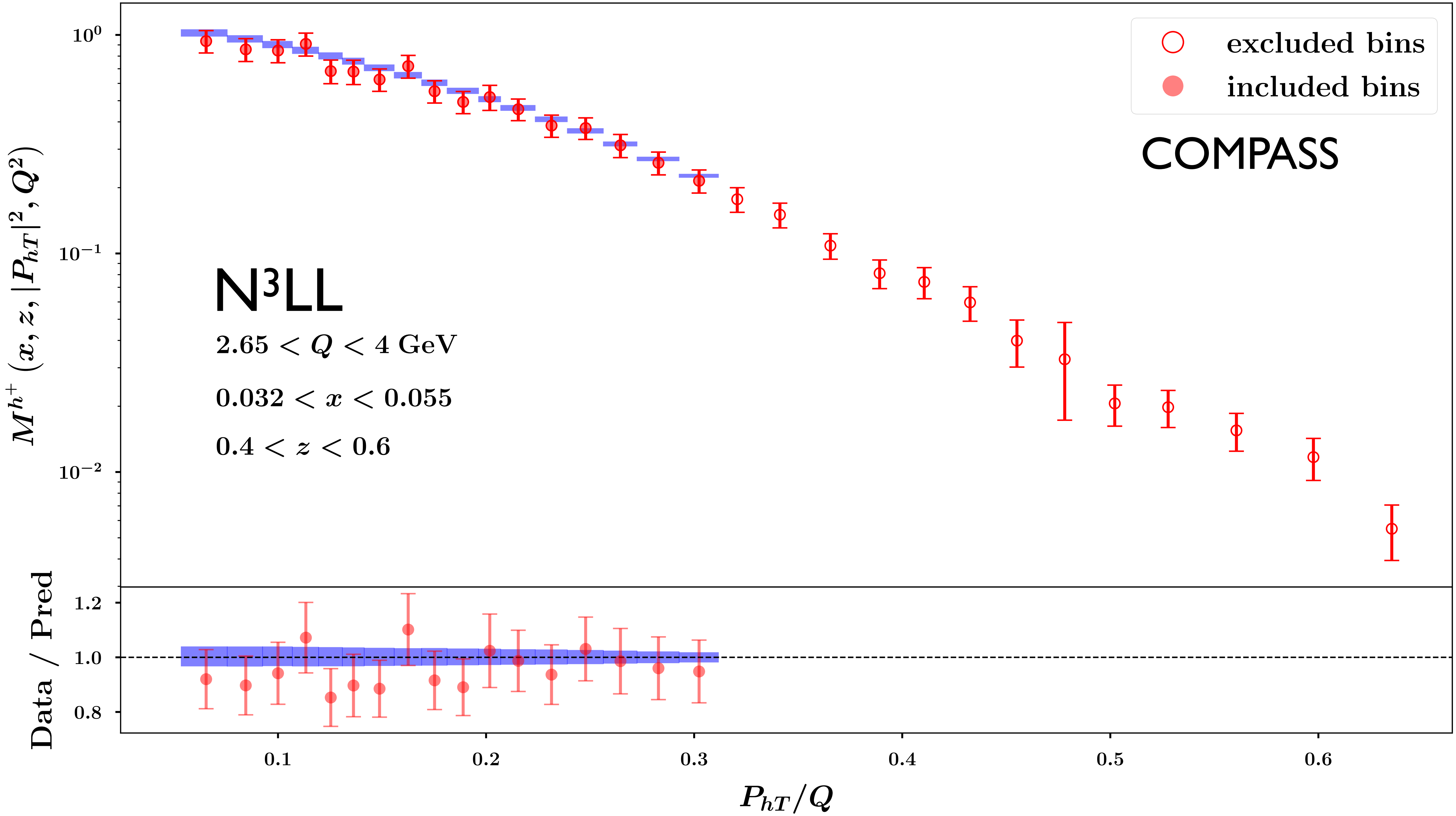

- Excellent agreement upon normalisation.

MAPTMD 2022

Fit quality: $\chi^2 \sim 1$

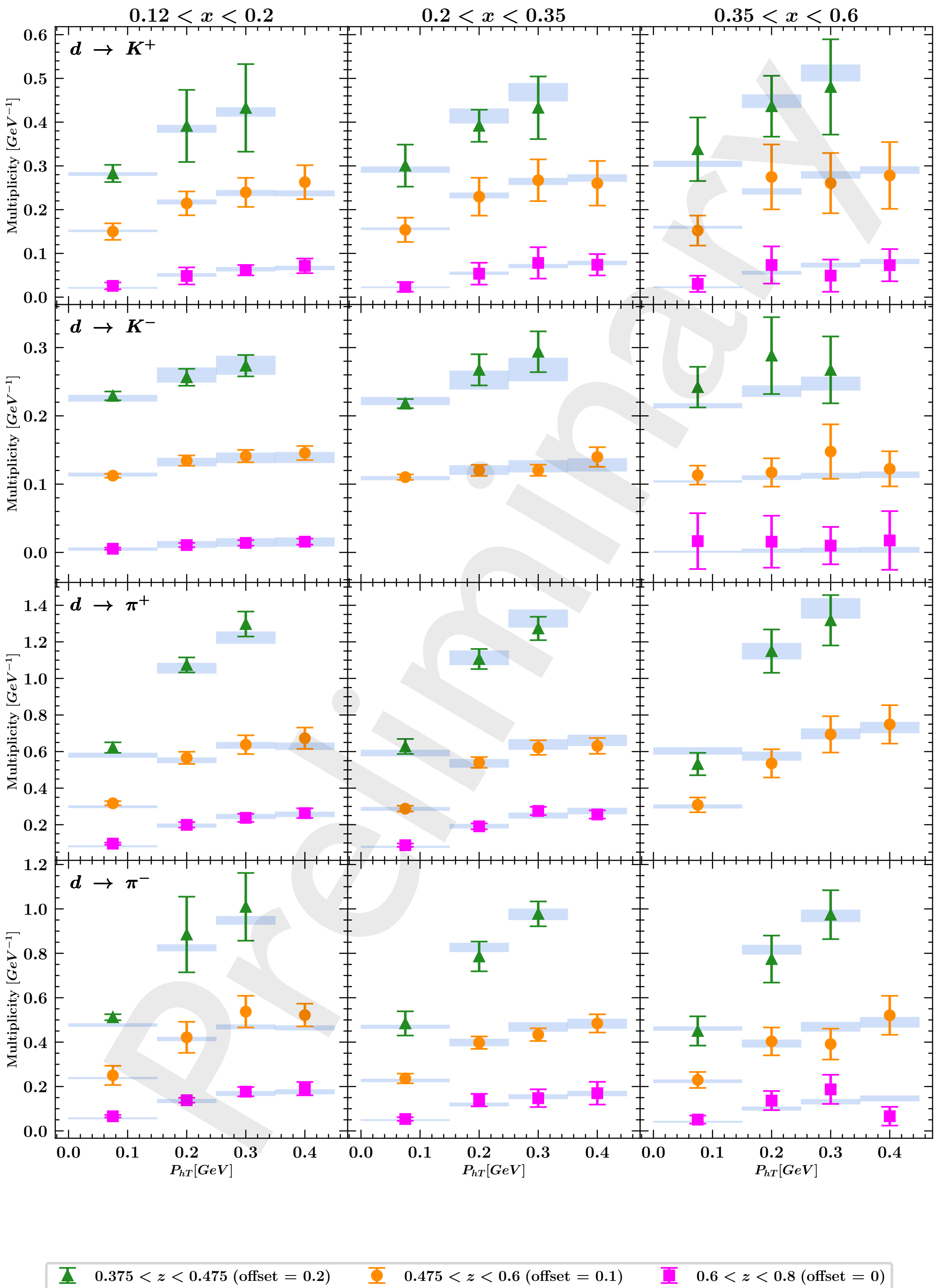

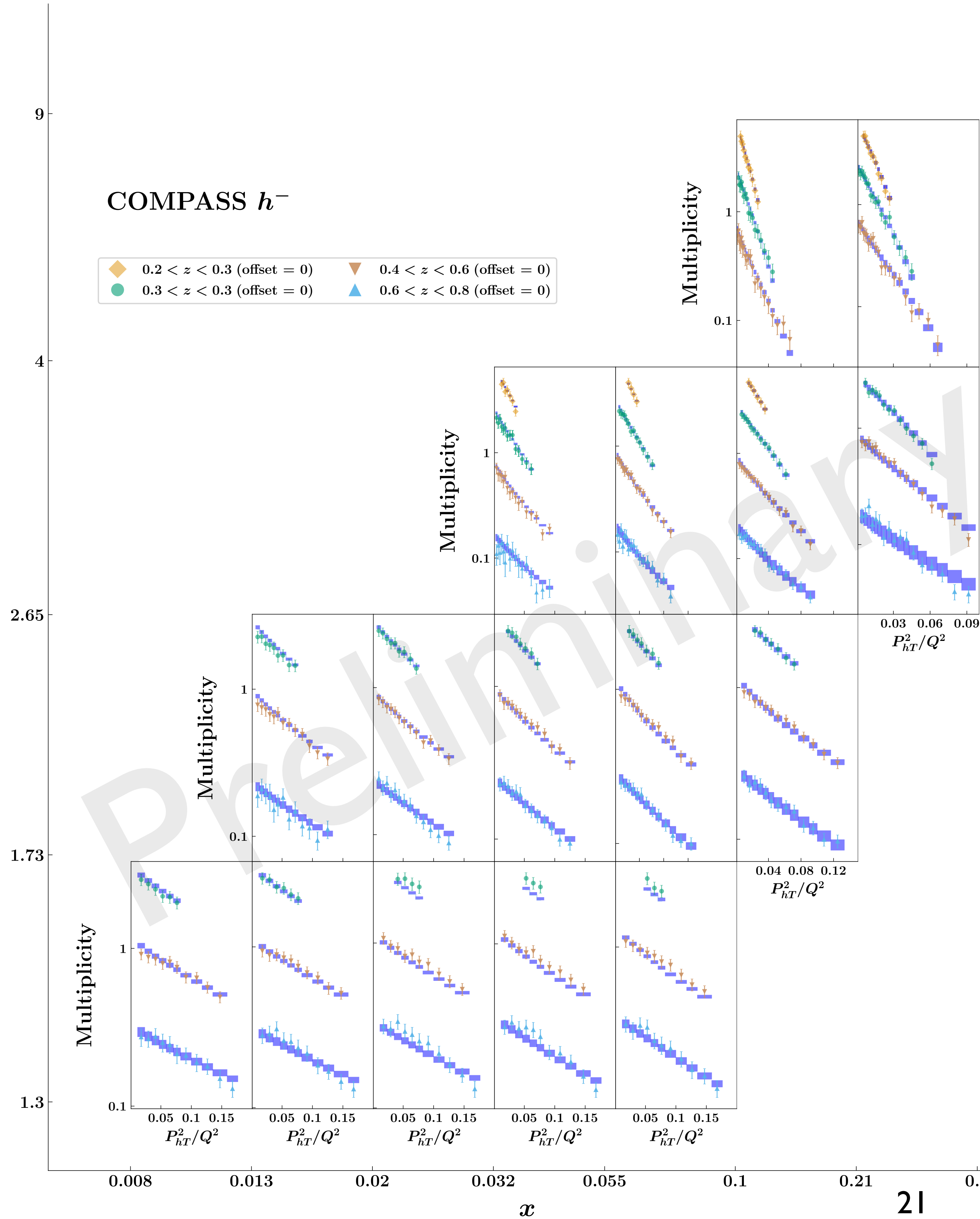

MAPTMD 2022

Fit quality: $\chi^2 \sim 1$

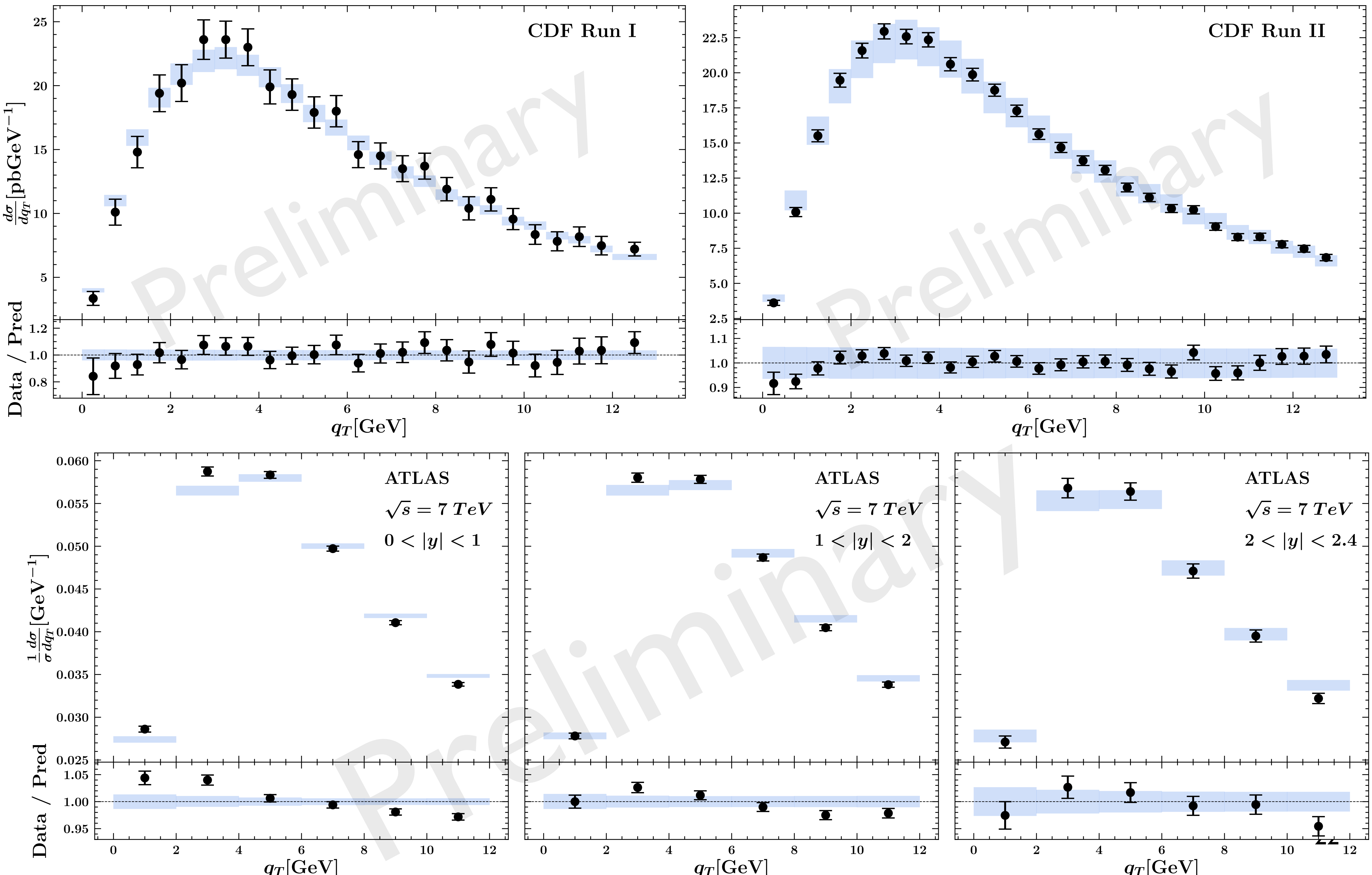

MAPTMD 2022

Collins-Soper kernel

$$D(b_T, \mu) = -K(b_*(b_T), \mu) - g_K(b_T)$$

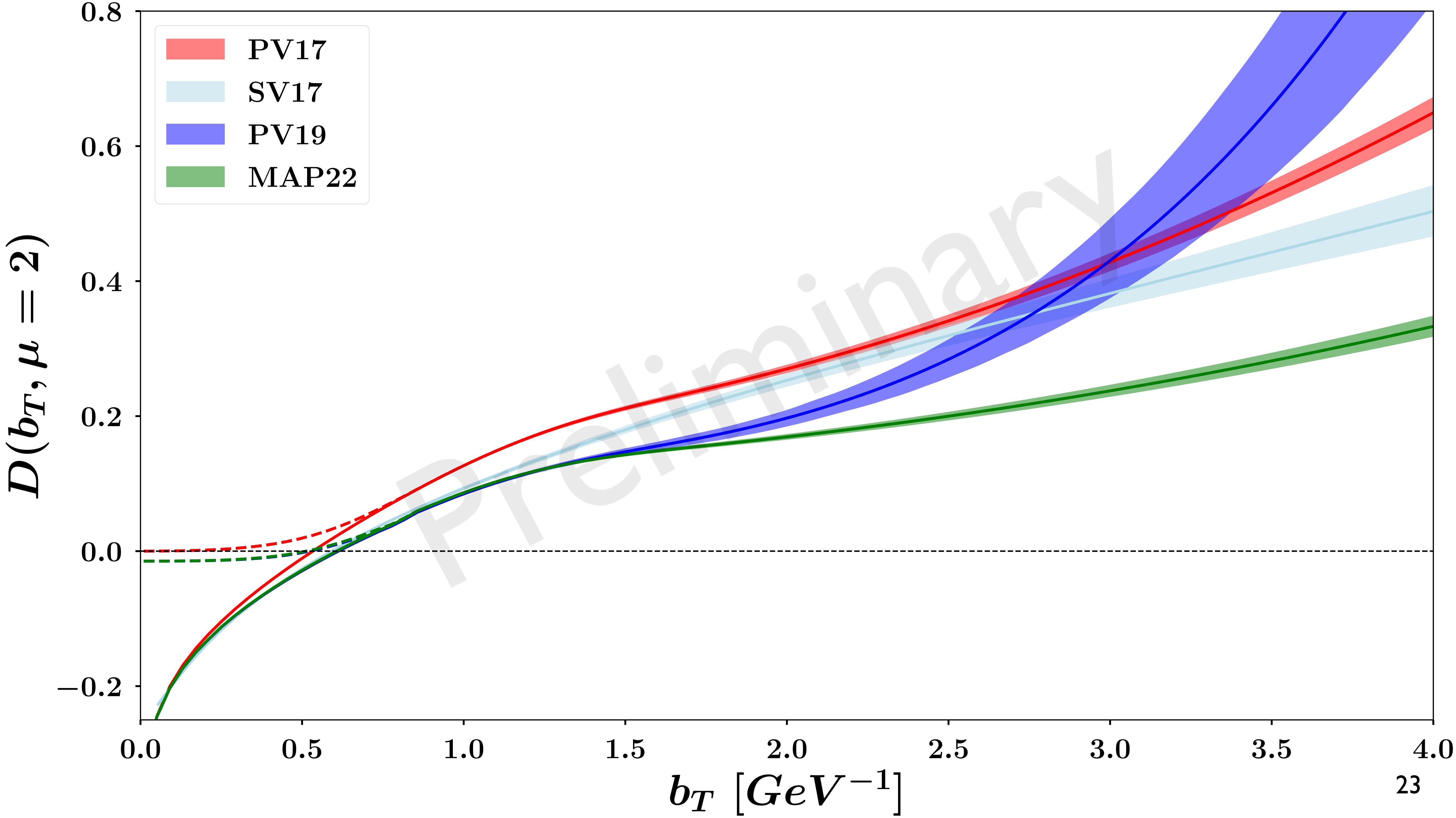

Conclusions

- **TMD factorisation** provides a valuable tool to descrive q_T distributions at small values of q_T (resummation of large logs),
  - written in terms of **TMD distributions,**
- Non-perturbative component of TMDs to be determined from **data**
- A lot of effort is being invested on the extraction of TMD PDFs and FFs:
  - tremendous progress made over the past few years,
  - wide and precise **datasets** (COMPASS, HERMES, LHC and Tevatron exps.),
  - more data to come from the LHC,
  - state-of-the-art **theoretical computation** moving to even higher accuracy.

Backup

Logarithmic counting

- TMD factorisation provides **resummation** of large logs $L = \log(q_T/Q)$:
  - implemented through the **Sudakov** form fact R.
- A **perturbative expansion** in powers of α_s of R would give:

One Sudakov for each TMD → R^2

$$R^{2} = \sum_{n=0}^{\infty} a_s^n \sum_{k=1}^{2n} \widetilde{S}^{(n,k)} L^k$$

Double-log expansion → $2n$

- that can be rearranged as:

$$R^2 = \sum_{m=0}^{\infty} R^2_{\mathrm{N^mLL}} \quad \text{with} \quad R^2_{\mathrm{N^mLL}} = \sum_{n=[m/2]}^{\infty} \widetilde{S}^{(n,2n-m)} a_s^n L^{2n-m}$$

Integer part of m/2

- Therefore, multiplying R by a power p of α_s gives:

$$a_s^p R^2_{\mathrm{N^mLL}} = \sum_{j=[(m+2p)/2]}^{\infty} \widetilde{S}^{(j-p,2j-(m+2p))} a_s^j L^{2j-(m+2p)} \sim R^2_{\mathrm{N^{m+2p}LL}}$$

- Bottom line: any additional power of α_s causes a shift of **two units** in the logarithmic ordering.

Pavia2019

Dataset

- DY data only:
  - fixed-target low-energy DY,
  - STAR data
  - LHC and Tevatron data,
  - 353 data points,
  - selection cut q_T / $Q < 0.2$.

Experiment	N_{dat}	Observable	$\sqrt{s}$ [GeV]	Q [GeV]	y or x_F	Lepton cuts	Ref.
E605	50	$Ed^3\sigma/d^3q$	38.8	7 - 18	$x_F = 0.1$	-	[79]
E288 200 GeV	30	$Ed^3\sigma/d^3q$	19.4	4 - 9	$y = 0.40$	-	[80]
E288 300 GeV	39	$Ed^3\sigma/d^3q$	23.8	4 - 12	$y = 0.21$	-	[80]
E288 400 GeV	61	$Ed^3\sigma/d^3q$	27.4	5 - 14	$y = 0.03$	-	[80]
STAR 510	7	$d\sigma/dq_T$	510	73 - 114	$\|y\| < 1$	$p_{T\ell} > 25$ GeV $\|\eta_\ell\| < 1$	-
CDF Run I	25	$d\sigma/dq_T$	1800	66 - 116	Inclusive	-	[81]
CDF Run II	26	$d\sigma/dq_T$	1960	66 - 116	Inclusive	-	[82]
D0 Run I	12	$d\sigma/dq_T$	1800	75 - 105	Inclusive	-	[83]
D0 Run II	5	$(1/\sigma)d\sigma/dq_T$	1960	70 - 110	Inclusive	-	[84]
D0 Run II (μ)	3	$(1/\sigma)d\sigma/dq_T$	1960	65 - 115	$\|y\| < 1.7$	$p_{T\ell} > 15$ GeV $\|\eta_\ell\| < 1.7$	[85]
LHCb 7 TeV	7	$d\sigma/dq_T$	7000	60 - 120	$2 < y < 4.5$	$p_{T\ell} > 20$ GeV $2 < \eta_\ell < 4.5$	[86]
LHCb 8 TeV	7	$d\sigma/dq_T$	8000	60 - 120	$2 < y < 4.5$	$p_{T\ell} > 20$ GeV $2 < \eta_\ell < 4.5$	[87]
LHCb 13 TeV	7	$d\sigma/dq_T$	13000	60 - 120	$2 < y < 4.5$	$p_{T\ell} > 20$ GeV $2 < \eta_\ell < 4.5$	[92]
CMS 7 TeV	4	$(1/\sigma)d\sigma/dq_T$	7000	60 - 120	$\|y\| < 2.1$	$p_{T\ell} > 20$ GeV $\|\eta_\ell\| < 2.1$	[88]
CMS 8 TeV	4	$(1/\sigma)d\sigma/dq_T$	8000	60 - 120	$\|y\| < 2.1$	$p_{T\ell} > 15$ GeV $\|\eta_\ell\| < 2.1$	[89]
ATLAS 7 TeV	6 6 6	$(1/\sigma)d\sigma/dq_T$	7000	66 - 116	$\|y\| < 1$ $1 < \|y\| < 2$ $2 < \|y\| < 2.4$	$p_{T\ell} > 20$ GeV $\|\eta_\ell\| < 2.4$	[93]
ATLAS 8 TeV on-peak	6 6 6 6 6 6	$(1/\sigma)d\sigma/dq_T$	8000	66 - 116	$\|y\| < 0.4$ $0.4 < \|y\| < 0.8$ $0.8 < \|y\| < 1.2$ $1.2 < \|y\| < 1.6$ $1.6 < \|y\| < 2$ $2 < \|y\| < 2.4$	$p_{T\ell} > 20$ GeV $\|\eta_\ell\| < 2.4$	[90]
ATLAS 8 TeV off-peak	4 8	$(1/\sigma)d\sigma/dq_T$	8000	46 - 66 116 - 150	$\|y\| < 2.4$	$p_{T\ell} > 20$ GeV $\|\eta_\ell\| < 2.4$	[90]
Total	353	-	-	-	-	-	-

Pavia2019

Kinematic coverage

$$x_{1,2} = \frac{Q}{\sqrt{s}} e^{\pm y}$$

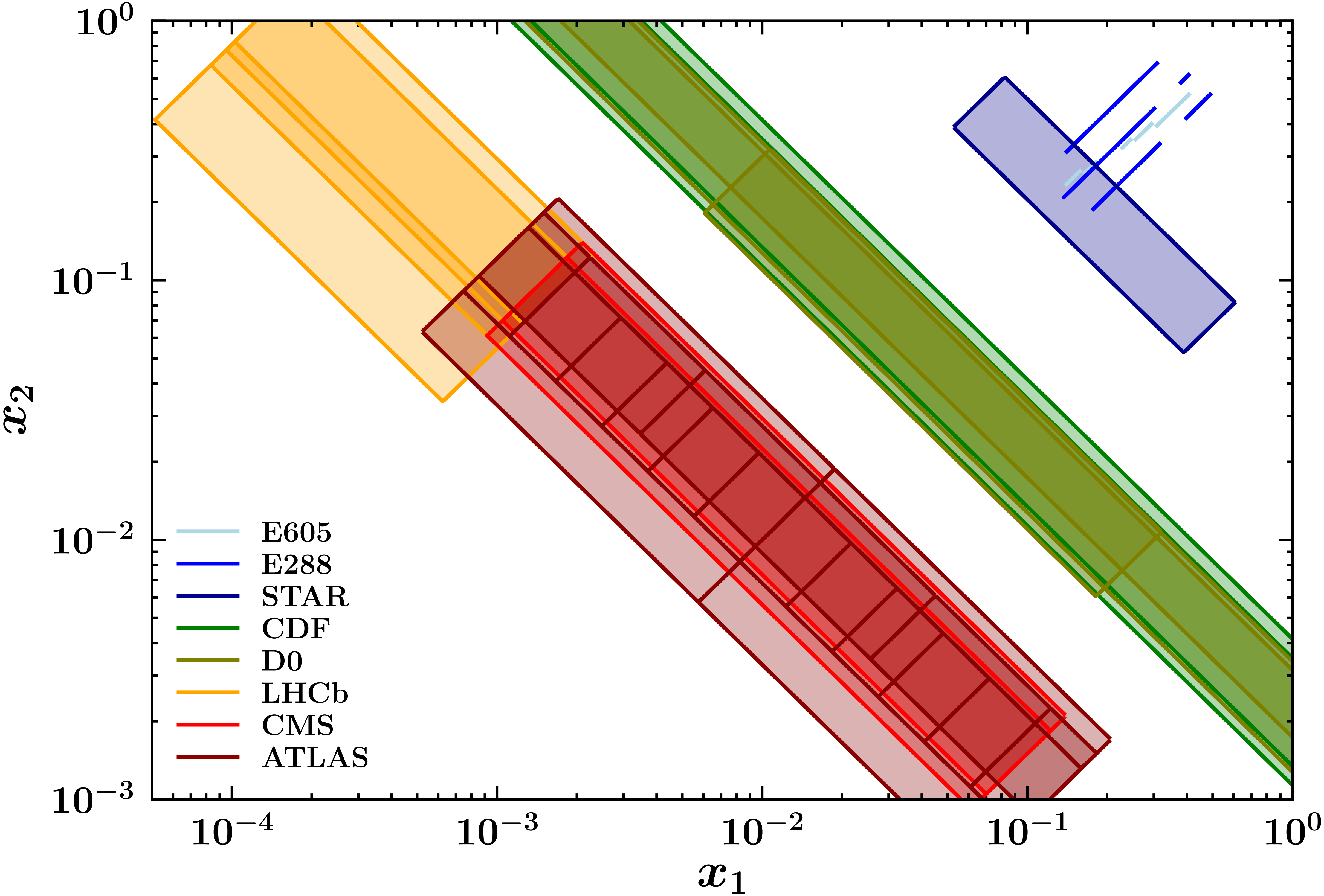

Pavia2019

Main settings

- b_* prescription:

$$b_*(b_T) = b_{\max}\left(\frac{1-e^{-b_T^4/b_{\max}^4}}{1-e^{-b_T^4/b_{\min}^4}}\right)^{1/4} \quad \text{with} \quad \begin{cases} b_{\max} = 2e^{-\gamma_E} \\ b_{\min} = b_{\max}/Q \end{cases}$$

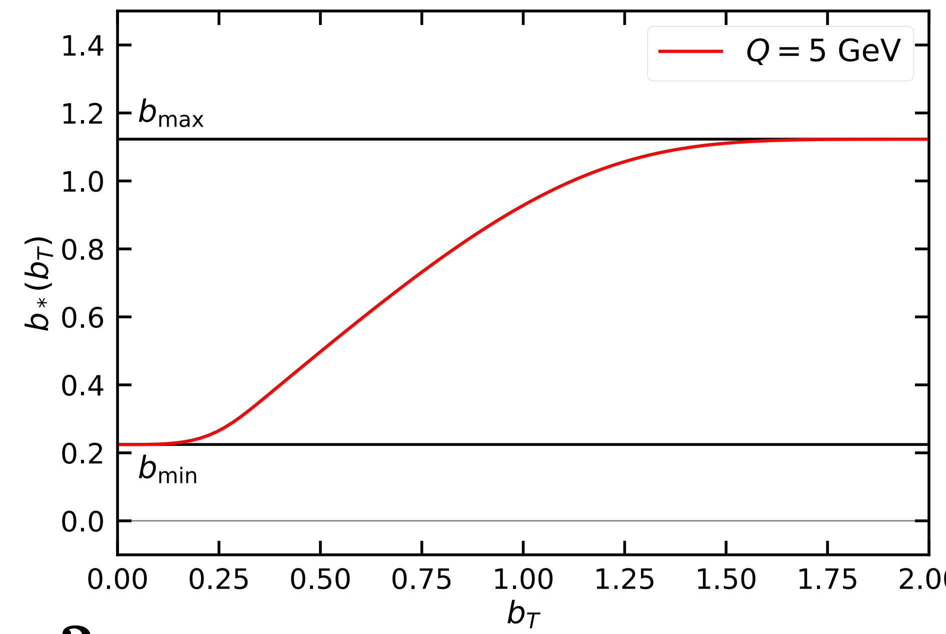

- Non-perturbative function f_{NP}:
  - evolution:

$$g_K(b_T) = -\left(g_2 + g_{2B} b_T^2\right)\frac{b_T^2}{2}$$

  - PDFs:

$$\widetilde{f}_{NP}(x, b_T) = \left[\frac{1-\lambda}{1+g_1(x)\frac{b_T^2}{4}} + \lambda \exp\left(-g_{1B}(x)\frac{b_T^2}{4}\right)\right]$$

$$g_1(x) = \frac{N_1}{x\sigma}\exp\left[-\frac{1}{2\sigma^2}\ln^2\left(\frac{x}{\alpha}\right)\right] \qquad g_{1B}(x) = \frac{N_{1B}}{x\sigma_B}\exp\left[-\frac{1}{2\sigma_B^2}\ln^2\left(\frac{x}{\alpha_B}\right)\right]$$

- **9 free parameters** to fit to data.
- Perturbative accuracies: **NLL', NNLL, NNLL', N^{3}LL**
- **Monte Carlo** method for the experimental error propagation.

Pavia2019

Fit quality

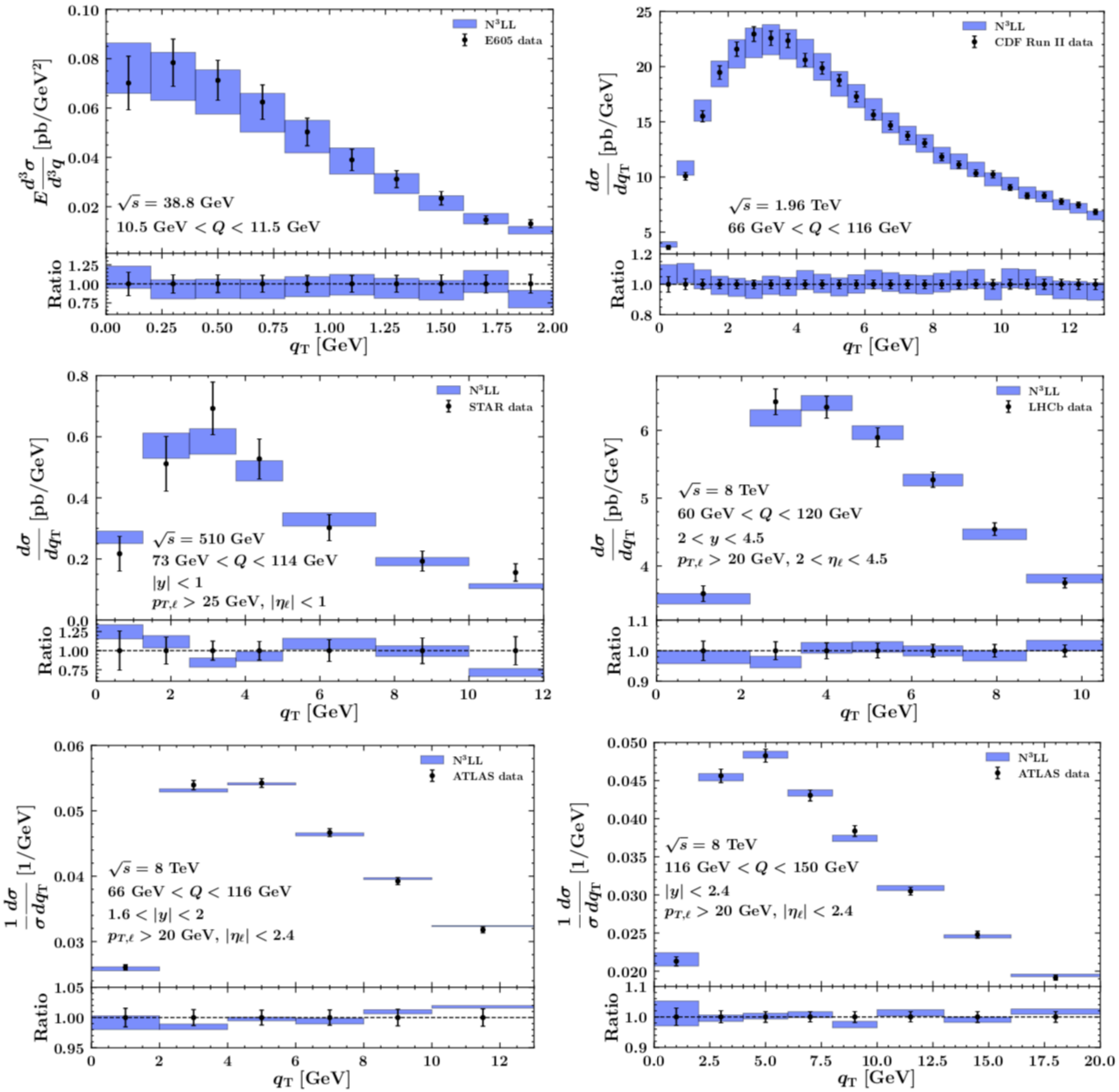

Experiment		χ^2_D/N_{dat}	χ^2_λ/N_{dat}	χ^2/N_{dat}
E605	7 GeV < Q < 8 GeV	0.419	0.068	0.487
	8 GeV < Q < 9 GeV	0.995	0.034	1.029
	10.5 GeV < Q < 11.5 GeV	0.191	0.137	0.328
	11.5 GeV < Q < 13.5 GeV	0.491	0.284	0.775
	13.5 GeV < Q < 18 GeV	0.491	0.385	0.877
E288 200 GeV	4 GeV < Q < 5 GeV	0.213	0.649	0.862
	5 GeV < Q < 6 GeV	0.673	0.292	0.965
	6 GeV < Q < 7 GeV	0.133	0.141	0.275
	7 GeV < Q < 8 GeV	0.254	0.014	0.268
	8 GeV < Q < 9 GeV	0.652	0.024	0.676
E288 300 GeV	4 GeV < Q < 5 GeV	0.231	0.555	0.785
	5 GeV < Q < 6 GeV	0.502	0.204	0.706
	6 GeV < Q < 7 GeV	0.315	0.063	0.378
	7 GeV < Q < 8 GeV	0.056	0.030	0.086
	8 GeV < Q < 9 GeV	0.530	0.017	0.547
	11 GeV < Q < 12 GeV	1.047	0.167	1.215
E288 400 GeV	5 GeV < Q < 6 GeV	0.312	0.065	0.377
	6 GeV < Q < 7 GeV	0.100	0.005	0.105
	7 GeV < Q < 8 GeV	0.018	0.011	0.029
	8 GeV < Q < 9 GeV	0.437	0.039	0.477
	11 GeV < Q < 12 GeV	0.637	0.036	0.673
	12 GeV < Q < 13 GeV	0.788	0.028	0.816
	13 GeV < Q < 14 GeV	1.064	0.044	1.107
STAR		0.782	0.054	0.836
CDF Run I		0.480	0.058	0.538
CDF Run II		0.959	0.001	0.959
D0 Run I		0.711	0.043	0.753
D0 Run II		1.325	0.612	1.937
D0 Run II (μ)		3.196	0.023	3.218
LHCb 7 TeV		1.069	0.194	1.263
LHCb 8 TeV		0.460	0.075	0.535
LHCb 13 TeV		0.735	0.020	0.755
CMS 7 TeV		2.131	0.000	2.131
CMS 8 TeV		1.405	0.007	1.412
ATLAS 7 TeV	0 < |y| < 1	2.581	0.028	2.609
	1 < |y| < 2	4.333	1.032	5.365
	2 < |y| < 2.4	3.561	0.378	3.939
ATLAS 8 TeV on-peak	0 < |y| < 0.4	1.924	0.337	2.262
	0.4 < |y| < 0.8	2.342	0.247	2.590
	0.8 < |y| < 1.2	0.917	0.061	0.978
	1.2 < |y| < 1.6	0.912	0.095	1.006
	1.6 < |y| < 2	0.721	0.092	0.814
	2 < |y| < 2.4	0.932	0.348	1.280
ATLAS 8 TeV off-peak	46 GeV < Q < 66 GeV	2.138	0.745	2.883
	116 GeV < Q < 150 GeV	0.501	0.003	0.504
Global		**0.88**	**0.14**	**1.02**

Pavia2019

Perturbative convergence

	NLL′	NNLL	NNLL′	N^{3}LL
Global χ^2	1126	571	379	360

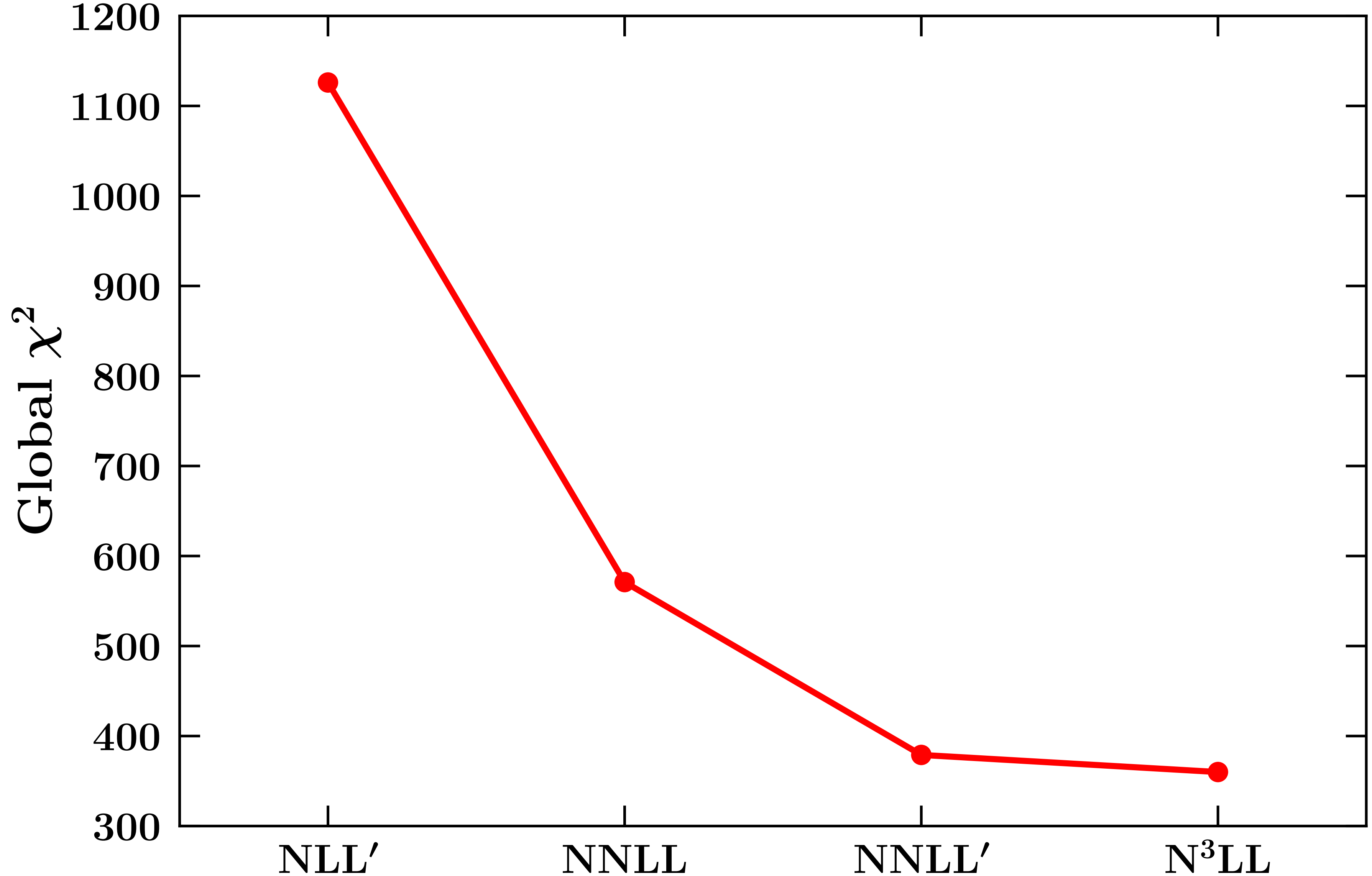

Pavia2019

Perturbative convergence

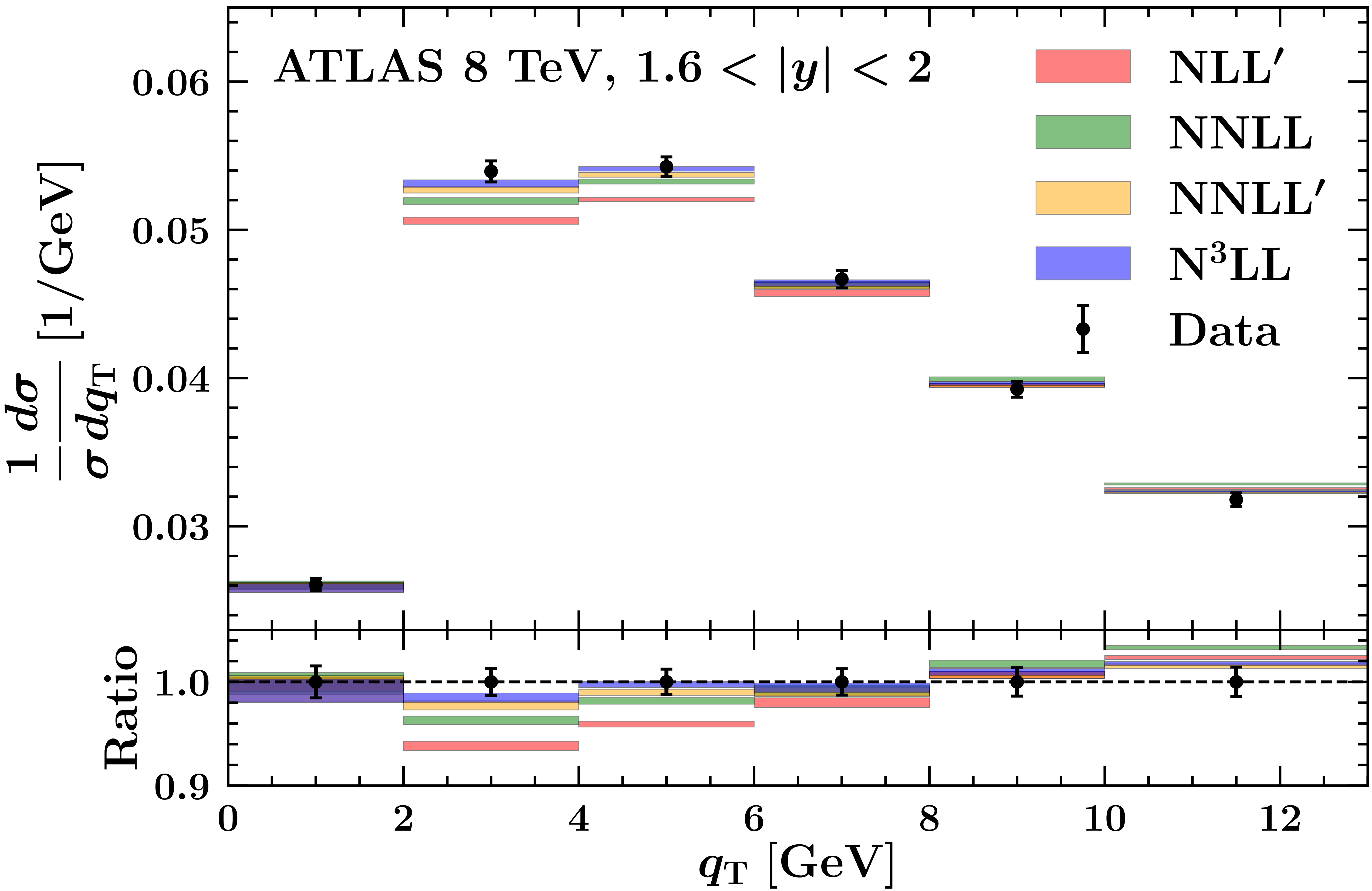

SV2019

Dataset

- Both DY and SIDIS data:
  - fixed-target low-energy DY,
  - PHENIX data,
  - LHC and Tevatron data,
  - HERMES and COMPASS,
  - 457 + 582 = 1039 data points.

DY

$$\delta \equiv \frac{\langle q_T \rangle}{\langle Q \rangle} < 0.1 \qquad \delta < 0.25 \quad \text{if} \quad \delta^2 < \sigma$$

Experiment	ref.	$\sqrt{s}$ [GeV]	Q [GeV]	y/x_F	fiducial region	$N_{\rm pt}$ after cuts
E288 (200)	[64]	19.4	4 - 9 in 1 GeV bins*	$0.1 < x_F < 0.7$	-	43
E288 (300)	[64]	23.8	4 - 12 in 1 GeV bins*	$-0.09 < x_F < 0.51$	-	53
E288 (400)	[64]	27.4	5 - 14 in 1 GeV bins*	$-0.27 < x_F < 0.33$	-	76
E605	[65]	38.8	7 - 18 in 5 bins*	$-0.1 < x_F < 0.2$	-	53
E772	[66]	38.8	5 - 15 in 8 bins*	$0.1 < x_F < 0.3$	-	35
PHENIX	[67]	200	4.8 - 8.2	$1.2 < y < 2.2$	-	3
CDF (run1)	[68]	1800	66 - 116	-	-	33
CDF (run2)	[69]	1960	66 - 116	-	-	39
D0 (run1)	[70]	1800	75 - 105	-	-	16
D0 (run2)	[71]	1960	70 - 110	-	-	8
D0 (run2)$_\mu$	[72]	1960	65 - 115	$\lvert y\rvert < 1.7$	$p_T > 15$ GeV $\lvert\eta\rvert < 1.7$	3
ATLAS (7TeV)	[45]	7000	66 - 116	$\lvert y\rvert < 1$ $1 < \lvert y\rvert < 2$ $2 < \lvert y\rvert < 2.4$	$p_T > 20$ GeV $\lvert\eta\rvert < 2.4$	15
ATLAS (8TeV)	[46]	8000	66 - 116	$\lvert y\rvert < 2.4$ in 6 bins	$p_T > 20$ GeV $\lvert\eta\rvert < 2.4$	30
ATLAS (8TeV)	[46]	8000	46 - 66	$\lvert y\rvert < 2.4$	$p_T > 20$ GeV $\lvert\eta\rvert < 2.4$	3
ATLAS (8TeV)	[46]	8000	116 - 150	$\lvert y\rvert < 2.4$	$p_T > 20$ GeV $\lvert\eta\rvert < 2.4$	7
CMS (7TeV)	[47]	7000	60 - 120	$\lvert y\rvert < 2.1$	$p_T > 20$ GeV $\lvert\eta\rvert < 2.1$	8
CMS (8TeV)	[48]	8000	60 - 120	$\lvert y\rvert < 2.1$	$p_T > 20$ GeV $\lvert\eta\rvert < 2.1$	8
LHCb (7TeV)	[73]	7000	60 - 120	$2 < y < 4.5$	$p_T > 20$ GeV $2 < \eta < 4.5$	8
LHCb (8TeV)	[74]	8000	60 - 120	$2 < y < 4.5$	$p_T > 20$ GeV $2 < \eta < 4.5$	7
LHCb (13TeV)	[75]	13000	60 - 120	$2 < y < 4.5$	$p_T > 20$ GeV $2 < \eta < 4.5$	9
Total						457

*Bins with $9 \lesssim Q \lesssim 11$ are omitted due to the Υ resonance.

SIDIS

$$\langle Q \rangle \geq 2\text{GeV} \qquad \delta \equiv \frac{\langle q_T \rangle}{\langle Q \rangle} < 0.25$$

Experiment	Reaction	ref.	Kinematics	$N_{\rm pt}$ after cuts
HERMES	$p \to \pi^+$	[58]	0.023<x<0.6 (6 bins) 0.2<z<0.8 (6 bins) 1.0<Q<$\sqrt{20}$GeV $W^2 > 10$GeV^2 0.1<y<0.85	24
	$p \to \pi^-$			24
	$p \to K^+$			24
	$p \to K^-$			24
	$D \to \pi^+$			24
	$D \to \pi^-$			24
	$D \to K^+$			24
	$D \to K^-$			24
COMPASS	$d \to h^+$	[59]	0.003<x<0.4 (8 bins) 0.2<z<0.8 (4 bins) 1.0<Q≃ 9GeV (5 bins)	195
	$d \to h^-$			195
Total				582

SV2019

Kinematic coverage

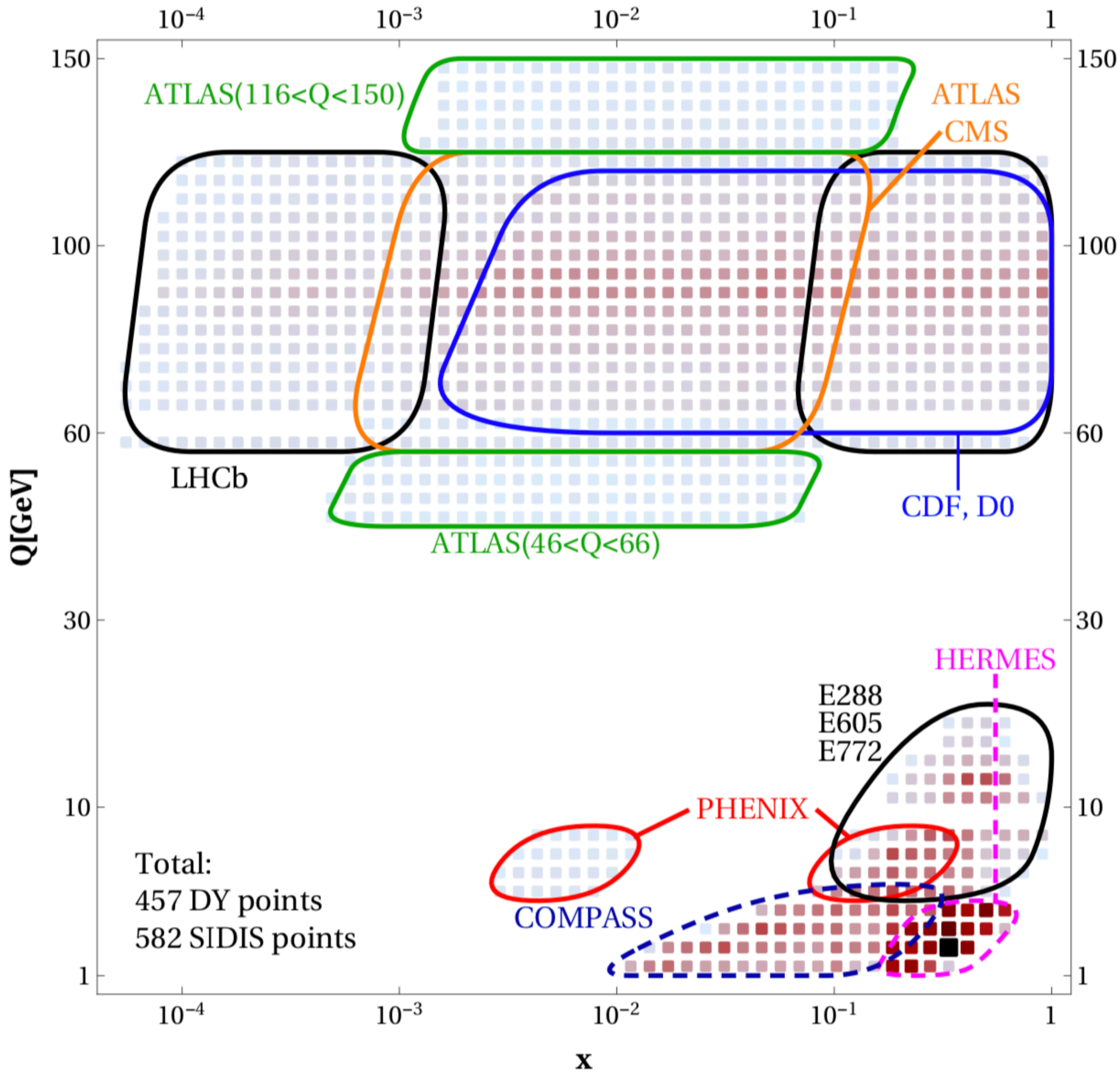

SV2019

Main settings

- b_* prescription: $$b_*(b_T) = \sqrt{\frac{b_T^2 B_{\rm NP}^2}{b_T^2 + B_{\rm NP}^2}}$$
- Non-perturbative function $f_{\rm NP}$:
  - evolution:
    $$g_K(b_T) = -c_0 b_T b_*(b_T) \quad \rightarrow \quad \begin{cases} -c_0 b_T^2 & \text{for } b_T \rightarrow 0 \\ -c_0 B_{\rm NP} b_T & \text{for } b_T \rightarrow \infty \end{cases}$$
  - PDFs and FFs:

$$f_{NP}(x,b) = \exp\left(-\frac{\lambda_1(1-x)+\lambda_2 x + x(1-x)\lambda_5}{\sqrt{1+\lambda_3 x^{\lambda_4}\boldsymbol{b}^2}}\boldsymbol{b}^2\right)$$

$$D_{NP}(x,b) = \exp\left(-\frac{\eta_1 z + \eta_2(1-z)}{\sqrt{1+\eta_3(\boldsymbol{b}/z)^2}}\frac{\boldsymbol{b}^2}{z^2}\right)\left(1+\eta_4\frac{\boldsymbol{b}^2}{z^2}\right)$$

- **11 free parameters** to fit to data.
- Perturbative accuracies: **NNLL'(NNLO), N³LL(-) (N³LO)**
- **Monte Carlo** method for the experimental error propagation.

SV2019

Fit quality

- Remarkably good total χ^2,
- DY and SIDIS data are separately well described,
- **Important achievement**:
  - simultaneous description of SIDIS and DY data within the same fit at high perturbative order.

		NNLO		N^3LO	
Data set	N_{pt}	χ^2/N_{pt}	$\langle d/\sigma\rangle$	χ^2/N_{pt}	$\langle d/\sigma\rangle$
CDF run1	33	0.66	8.4%	0.67	7.8%
CDF run2	39	1.28	2.8%	1.41	2.1%
D0 run1	16	0.72	0.1%	0.78	-0.5%
D0 run2	8	1.38	-	1.64	-
D0 run2 (μ)	3	0.62	-	0.69	-
Tevatron total	99	0.97		1.06	
ATLAS 7TeV 0.0<|y|<1.0	5	1.66	-	0.81	-
ATLAS 7TeV 1.0<|y|<2.0	5	5.94	-	4.09	-
ATLAS 7TeV 2.0<|y|<2.4	5	1.49	-	1.26	-
ATLAS 8TeV 0.0<|y|<0.4	5	2.51	3.5%	3.40	2.8%
ATLAS 8TeV 0.4<|y|<0.8	5	2.95	3.5%	3.03	2.7%
ATLAS 8TeV 0.8<|y|<1.2	5	1.30	3.7%	1.45	2.9%
ATLAS 8TeV 1.2<|y|<1.6	5	2.03	4.2%	1.53	3.4%
ATLAS 8TeV 1.6<|y|<2.0	5	1.47	4.9%	0.70	4.1%
ATLAS 8TeV 2.0<|y|<2.4	5	2.64	5.6%	2.10	4.8%
ATLAS 8TeV 46<Q<66GeV	3	0.31	1.1%	0.31	0.2%
ATLAS 8TeV 116<Q<150GeV	7	0.84	1.9%	0.97	1.2%
ATLAS total	55	2.12		1.82	
CMS 7TeV	8	1.25	-	1.24	-
CMS 8TeV	8	0.77	-	0.76	-
CMS total	16	1.01		1.00	
LHCb 7TeV	8	2.68	5.8%	2.37	5.2%
LHCb 8TeV	7	4.81	5.8%	4.16	5.1%
LHCb 13TeV	9	0.91	6.4%	0.81	5.7%
LHCb total	24	2.63		2.31	
High energy DY total	194	1.51		1.42	
PHE200	3	0.28	0.2%	0.29	-0.3%
E228-200	43	1.00	35.7%	1.12	35.0%
E228-300	53	0.90	29.2%	1.01	28.3%
E228-400	76	0.86	20.6%	0.96	19.5%
E772	35	1.84	9.5%	1.91	8.5%
E605	53	0.57	21.3%	0.60	20.1%
Low energy DY total	263	0.96		1.04	
HERMES ($p\to\pi^+$)	24	2.20	1.7%	3.06	2.2%
HERMES ($p\to\pi^-$)	24	1.12	0.6%	1.45	0.9%
HERMES ($p\to K^+$)	24	0.71	-0.1%	0.66	0.0%
HERMES ($p\to K^-$)	24	0.69	0.0%	0.66	0.0%
HERMES ($d\to\pi^+$)	24	0.57	0.3%	0.78	0.8%
HERMES ($d\to\pi^-$)	24	0.74	0.5%	0.96	0.7%
HERMES ($d\to K^+$)	24	0.52	-0.1%	0.53	0.0%
HERMES ($d\to K^-$)	24	1.27	0.0%	1.17	0.1%
HERMES total	192	0.98		1.16	
COMPASS ($d\to h^+$)	195	0.61	3.3%	0.76	5.1%
COMPASS ($d\to h^-$)	195	0.68	-2.3%	0.92	-0.5%
COMPASS total	390	0.65		0.84	
SIDIS total	582	0.76		0.95	
Total	**1039**	**0.95**		**1.06**	

SV2019

Fit quality

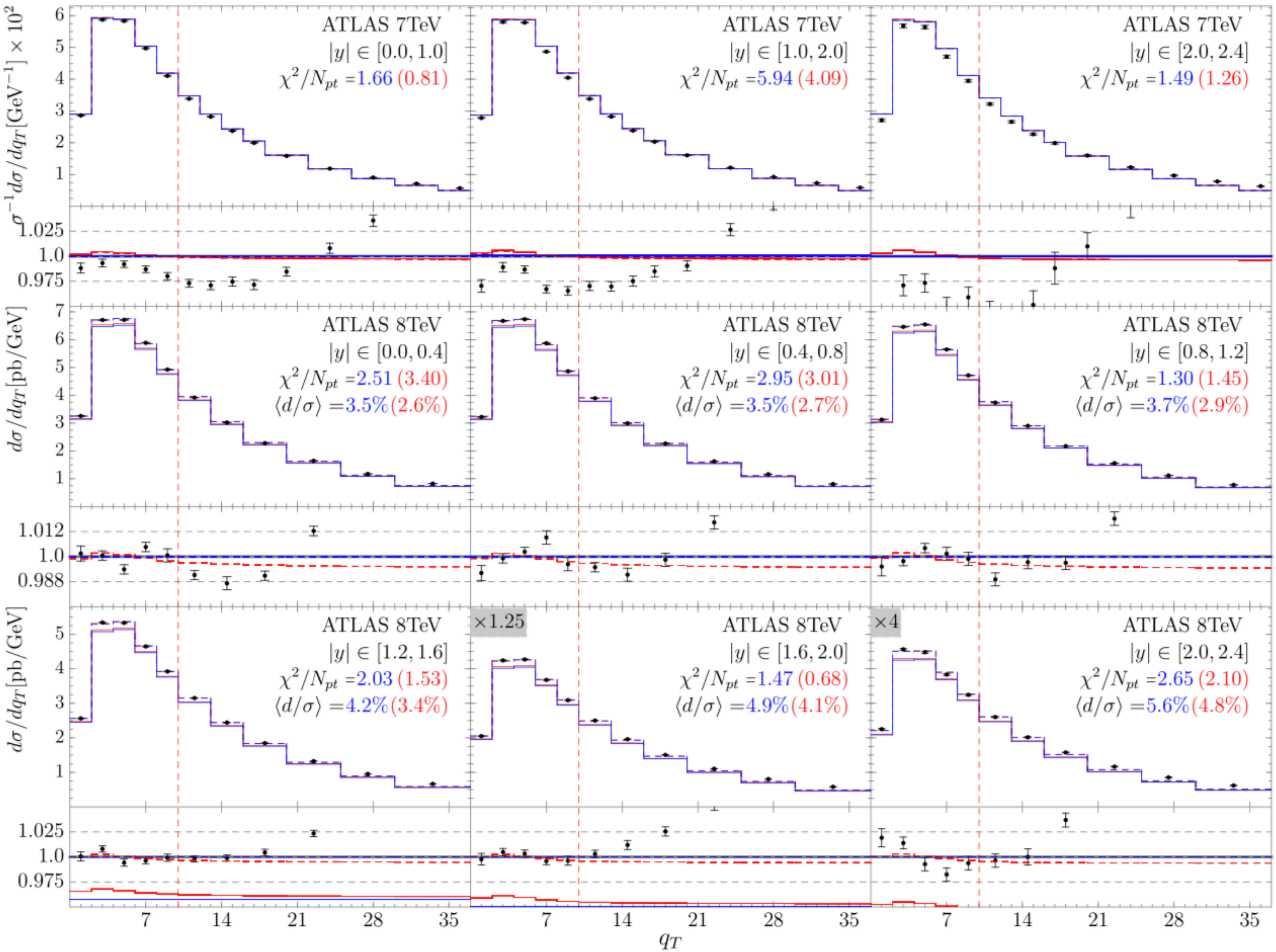

SV2019

Fit quality

COMPASS

$z^2 \times M(z, p_T)$

$d \to h^+$